

# Matching $Z \rightarrow$ Hadrons at NNLO with Sector Showers

---

Basem Kamal El-Menoufi,<sup>1</sup> Christian T. Preuss,<sup>2</sup> Ludovic Scyboz,<sup>1</sup> Peter Skands<sup>1</sup>

<sup>1</sup>*School of Physics & Astronomy, Monash University, Clayton VIC-3800, Australia*

<sup>2</sup>*University of Wuppertal, Department of Physics, DE-42119 Wuppertal, Germany*

**ABSTRACT:** We consider leading-colour 2-, 3- and 4-jet rates in hadronic  $Z$ -boson decay to derive matching conditions at next-to-next-to-leading order in the sectorised VINCIA parton shower. In particular, we present a full subtraction-based calculation of the matching coefficient required to obtain the NLO 3-jet rate. This is achieved through a judicious choice of the counter-terms, which optimises the numerical evaluation of the subtracted double-real matrix element. We additionally give a consistent prescription for incorporating interference effects due to multiple Born states. Finally, we briefly comment on higher-order uncertainty estimates.

**KEYWORDS:** QCD, Parton Shower, NNLO, Matching, LEP

*For the purpose of Open Access, the authors have applied a CC BY public copyright licence to any Author Accepted Manuscript (AAM) version arising from this submission.*

---

## Contents

<b>1</b>	<b>Introduction</b>	<b>1</b>
<b>2</b>	<b>Fixed-order jet rates in Z decay</b>	<b>2</b>
<b>3</b>	<b>NLO 3-jet matching</b>	<b>4</b>
3.1	NLO 3-jet matching with sector subtraction	10
3.1.1	Summary of matching by sector subtraction	14
3.1.2	Bootstrapping the $B$ sector	14
3.1.3	The $v^{\text{NLO}}$ factor	15
3.2	The $N_F$ piece	16
3.2.1	Multiple interfering Born states	17
3.2.2	Sector resolution for $g \rightarrow q\bar{q}$ splittings	20
3.2.3	Sector subtraction for $g \rightarrow q\bar{q}$	20
3.3	The renormalisation terms	21
<b>4</b>	<b>Uncertainties</b>	<b>23</b>
<b>5</b>	<b>Summary &amp; Outlook</b>	<b>24</b>
<b>A</b>	<b>The function <math>\mathcal{F}(x)</math></b>	<b>25</b>
<b>B</b>	<b>Virtual corrections</b>	<b>25</b>
<b>C</b>	<b>NLO 3-jet matching with global subtraction</b>	<b>26</b>

---

## 1 Introduction

With ever-increasing precision on the side of collider experiments, it has become imperative to address the accuracy of ingredients used in Monte Carlo event generators (MCEG), in particular their parton-shower component. The latter is responsible for generating the radiation pattern of QCD from the energetic scale of the hard collision down to the hadronisation scale, and a precise description of this extra radiation is crucial for the interpretation of data at the Large Hadron Collider (LHC). Recently, considerable efforts to improve the parton-shower component of MCEG's have led to the advent of next-to-leading logarithmic (NLL) accurate showers [1–9], with a clear path towards full NNLL accuracy [10, 11].

In addition to all-order resummation, the shower needs to be matched to fixed-order calculations to correctly describe hard (resolved) radiation. Two well-known schemes are used to match parton showers at next-to-leading order (NLO): MC@NLO [12] and

POWHEG [13, 14], along with a few more recent proposals [15–17]. Next-to-next-to-leading order (NNLO) matching is more involved, and several approaches have been applied to specific processes of interest at the LHC, i.e. NNLOPS [18], UN<sup>2</sup>LOPS [19, 20], as well as MiNNLO<sub>PS</sub> [21] and GENEVA [22].

Early on, it was realised in ref. [23] that a mismatch between the evolution variable of the hardest-emission generator and the subsequent shower can lead to a under- or over-counting of phase space. Ref. [24] later examined the interplay between matching and logarithmic accuracy at NLO in final-state showers. This study established that extra care is needed in the “handover” between an external phase-space generator, responsible for the first emission(s), and the parton shower: often such a construction requires that emissions in double-counted phase-space regions be vetoed [13, 24, 25]. Therefore, it is advantageous to use the parton shower itself as a phase-space generator for the *matched* emissions [26, 27]. That is the strategy we adopt in this paper within the VINCIA sector shower framework [28–31].

Sector showers, as implemented e.g. in VINCIA, facilitate the application of tree-level matrix-element corrections. This is due to the fact that each  $n$ -parton phase-space point can only be reached via a single shower path. Recently, a proposal for matching sectorised parton showers to NNLO perturbative accuracy was presented by several of us in ref. [32]. Here, we derive explicit expressions for the matching coefficients required for hadronic  $Z$  decays, fully differentially in each of the 2-, 3-, and 4-parton phase spaces. These are accompanied by an implementation of our subtraction method in C++ for numerical evaluation.

In sec. 2, we summarise the calculation of ARCLUS [33] jet rates at fixed order for hadronic  $Z$  decays and establish a notation that will be convenient for the remainder of the paper. In sec. 3 we derive the explicit forms of the  $\mathcal{O}(\alpha_s^2)$  matching terms at the 3-jet level. Sec. 3.1 describes the subtraction procedure that we implement in order to evaluate the NLO 3-jet matching coefficient. In sec. 3.2 we provide the  $N_F$  contribution, as well as a consistent treatment of the interference between different Born processes. We give some recommendations on evaluating uncertainties associated with uncontrolled higher-order terms in sec. 4, and finally conclude in sec. 5. Appendices A–C include some auxiliary formulae and alternative prescriptions beyond those covered in the main text.

## 2 Fixed-order jet rates in $Z$ decay

We start by considering jet rates as defined with an infrared- and collinear-safe, deterministic, sequential jet algorithm. For this class of observables, the  $\mathcal{O}(\alpha_s^2)$  perturbative expansions for the *fully-differential* inclusive 2-, 3-, and 4-jet rates in  $Z$  decay (suppressing overall energy-momentum-conserving  $\delta$  functions) are, respectively:

NNLO 2-Jet Rate: (2.1)

$$\begin{aligned} \frac{m_Z}{8\pi^4} \frac{d^2\Gamma}{d\Phi_2} &= |M_2^0|^2 + 2\text{Re}[M_2^1 M_2^{0*}] + \int d\Phi_3 |M_3^0|^2 \delta^{(2)}(\Phi_2 - \hat{\Phi}_2(\Phi_3)) \\ &+ |M_2^1|^2 + 2\text{Re}[M_2^2 M_2^{0*}] + \int d\Phi_3 2\text{Re}[M_3^1 M_3^{0*}] \delta^{(2)}(\Phi_2 - \hat{\Phi}_2(\Phi_3)) \\ &+ \int d\Phi_4 |M_4^0|^2 \delta^{(2)}(\Phi_2 - \hat{\Phi}_2(\Phi_4)) + \mathcal{O}(\alpha_s^3), \end{aligned}$$

NLO 3-Jet Rate: (2.2)

$$\frac{m_Z}{8\pi^4} \frac{d^5\Gamma}{d\Phi_3} = |M_3^0|^2 + 2\text{Re}[M_3^1 M_3^{0*}] + \int d\Phi_4 |M_4^0|^2 \delta^{(5)}(\Phi_3 - \hat{\Phi}_3(\Phi_4)) + \mathcal{O}(\alpha_s^3),$$

LO 4-Jet Rate: (2.3)

$$\frac{m_Z}{8\pi^4} \frac{d^8\Gamma}{d\Phi_4} = |M_4^0|^2 + \mathcal{O}(\alpha_s^3),$$

where we have left the dependence of the matrix elements on the respective  $n$ -parton phase spaces implicit, and denote the clustering prescription (a.k.a. clustering map) of the jet algorithm by

$$\hat{\Phi}_{n-m}(\Phi_n). \quad (2.4)$$

Note that, for  $m \geq 2$  we shall assume simple iteration of single clusterings unless otherwise specified.

These are the expressions we shall seek to match to fixed-order expansions of parton-shower rates below. To make the notation less cumbersome, we adopt a POWHEG-inspired notation with  $\mathbf{B}_n$  the lowest-order matrix element for  $n$  partons,  $\mathbf{V}_n$  the sum of the integrated real and virtual contributions at NLO, and similarly  $\mathbf{W}_n$  for the NNLO contributions. With this notation, the terms in the above equations are:

$$\mathbf{B}_2 = |M_2^0|^2, \quad (2.5)$$

$$\mathbf{B}_3 = |M_3^0|^2, \quad (2.6)$$

$$\mathbf{B}_4 = |M_4^0|^2, \quad (2.7)$$

$$\mathbf{V}_2 = 2\text{Re}[M_2^1 M_2^{0*}] + \int d\Phi_3 |M_3^0|^2 \delta^{(2)}(\Phi_2 - \hat{\Phi}_2(\Phi_3)), \quad (2.8)$$

$$\mathbf{V}_3 = 2\text{Re}[M_3^1 M_3^{0*}] + \int d\Phi_4 |M_4^0|^2 \delta^{(5)}(\Phi_3 - \hat{\Phi}_3(\Phi_4)), \quad (2.9)$$

$$\begin{aligned} \mathbf{W}_2 &= |M_2^1|^2 + 2\text{Re}[M_2^2 M_2^{0*}] + \int d\Phi_3 2\text{Re}[M_3^1 M_3^{0*}] \delta^{(2)}(\Phi_2 - \hat{\Phi}_2(\Phi_3)) \\ &+ \int d\Phi_4 |M_4^0|^2 \delta^{(2)}(\Phi_2 - \hat{\Phi}_2(\Phi_4)). \end{aligned} \quad (2.10)$$

We also define a variant of  $\mathbf{V}_3$  in which the 4-parton integral only includes *ordered* clustering sequences, i.e. for which the jet clustering measure evaluated on the clustered 3-parton state

is larger than that evaluated on the 4-parton state,

$$V_3^O = 2\text{Re}[M_3^1 M_3^{0*}] + \int_{t_3 > t_4} d\Phi_4 |M_4^0|^2 \delta^{(5)}(\Phi_3 - \hat{\Phi}_3(\Phi_4)), \quad (2.11)$$

with  $t_n = t(\Phi_n)$  the jet-clustering resolution.

We emphasise that the rates in eqs. (2.1)–(2.3) are *fully differential* in each of the respective phase spaces, hence it should not matter which specific jet algorithm we pick as the basis for deriving the matching equations. In sec. 3 we exploit this freedom to make a choice that will be particularly convenient for us.

Note also that, in addition to the implicit dependence on the phase-space variables,  $\Phi_n$ , the amplitudes will also in general contain one or more powers of the renormalised coupling evaluated at a specific scale  $\mu_M$ ,

$$|M_n|^2 \equiv |M_n(\Phi_n; \mu_M)|^2. \quad (2.12)$$

For a process as simple as  $Z$  decay, it is trivial to match a probability-conserving shower to the inclusive NNLO rate, simply by using the full NNLO expression for the total width,  $\propto B_2 + V_2 + W_2$ . Since the matching prescription we define preserves this property of strict unitarity, we shall not comment on the inclusive NNLO normalisation further, though we do return to it in the context of ambiguities that enter at  $\mathcal{O}(\alpha_s^3)$ , in sec. 4.

Below, we shall also need the explicit forms of  $B_2$  and  $V_2$ , the former of which is just the tree-level squared matrix element for  $Z$  decay and the latter of which is the well-known NLO correction [34],

$$V_2 = \frac{\alpha_s(m_Z^2)}{\pi} B_2. \quad (2.13)$$

### 3 NLO 3-jet matching

Here, we examine the 3-jet rate in the ARCLUS algorithm [33]. Since our sector shower represents an inverse of that clustering procedure, this will simplify the derivation of the matching equations. The ARCLUS algorithm performs  $3 \mapsto 2$  clusterings according to a resolution variable  $t_n$ . To simplify the discussion, let us consider the  $n$ -parton state  $\bar{q}g_1 \dots g_{n-2}q$  (we will come back to  $g \rightarrow q\bar{q}$  splittings in sec. 3.2.1). ARCLUS computes the following “transverse momentum”,

$$t_{[j]/ik} = \frac{s_{ij}s_{jk}}{s_{ijk}}, \quad (3.1)$$

where for our purposes  $i$ ,  $j$ , and  $k$  are colour-connected. The jet resolution is then defined as:

$$t_n = \min_{[j]} t_{[j]/ik}(\Phi_n), \quad (3.2)$$

for the smallest value of  $t_{[j]}$  in an  $n$ -parton configuration.<sup>1</sup>

---

<sup>1</sup>The sector resolution variable appropriate for  $g \rightarrow q\bar{q}$  splittings is discussed in sec. 3.2.

For a parton shower starting from 2-parton configurations normalised to the inclusive NNLO rate, the differential rate of 3-parton configurations is, naively,<sup>2</sup>

$$\frac{m_Z}{8\pi^4} \frac{d^5\Gamma}{d\Phi_3} = (\mathbf{B}_2 + \mathbf{V}_2 + \mathbf{W}_2) \Delta_2(m_Z^2, t_3) A_{2\rightarrow 3}, \quad (3.3)$$

with  $A_{2\rightarrow 3}$  the  $2 \rightarrow 3$  antenna function of the shower (on which we shall impose matching conditions below) and  $\Delta_2$  the corresponding no-emission probability. We have again left the phase-space dependence implicit, understanding that terms with a subscript  $n$  depend on a corresponding  $n$ -parton phase space. For example,<sup>3</sup>

$$\mathbf{B}_2 \equiv \mathbf{B}_2(\hat{\Phi}_2(\Phi_3)), \quad (3.4)$$

$$\Delta_2(m_Z^2, t_3) \equiv \Delta_2(\hat{\Phi}_2(\Phi_3), m_Z^2, t_3(\Phi_3)), \quad (3.5)$$

$$A_{2\rightarrow 3} \equiv A_{2\rightarrow 3}(\hat{\Phi}_2(\Phi_3), \Phi_3). \quad (3.6)$$

For a shower matched to 3-parton matrix elements at  $\mathcal{O}(\alpha_s)$  or  $\mathcal{O}(\alpha_s^2)$  respectively, the emission densities must be given by

$$\mathbf{B}_2 A_{2\rightarrow 3}^{\text{LO}} = \mathbf{B}_3 + \mathcal{O}(\alpha_s^2), \quad (3.7)$$

$$(\mathbf{B}_2 + \mathbf{V}_2) (1 + \Delta_2^1(m_Z^2, t_3)) A_{2\rightarrow 3}^{\text{NLO}} = \mathbf{B}_3 + \mathbf{V}_3 + \mathcal{O}(\alpha_s^3), \quad (3.8)$$

where the superscript 1 on  $\Delta_2^1$  indicates the first-order term in the expansion of the shower no-emission probability,

$$\Delta_2^1(m_Z^2, t_3) = - \int_{t_3}^{m_Z^2} d\Phi_3 A_{2\rightarrow 3} \delta^{(2)}(\Phi_2 - \hat{\Phi}_2(\Phi_3)). \quad (3.9)$$

Solving eq. (3.7) for the antenna function yields the LO matching condition [35],

$$A_{2\rightarrow 3}^{\text{LO}} = \frac{\mathbf{B}_3}{\mathbf{B}_2} + \mathcal{O}(\alpha_s^2), \quad (3.10)$$

where we note that the ratio  $\mathbf{B}_3/\mathbf{B}_2$  for  $Z$  decay is identical to the GGG antenna function  $A_3^0$  [36] (modulo the colour and coupling factor). This is also the radiation function that would be employed in first-order MECs [35] or POWHEG [14] for  $Z$  decay.

Similarly, using eq. (3.8) yields *provisional* NLO matching conditions for  $A_{2\rightarrow 3}^{\text{NLO}}$ ,

$$A_{2\rightarrow 3}^{\text{NLO}} = \frac{\mathbf{B}_3 (1 - \Delta_2^1(m_Z^2, t_3)) + \mathbf{V}_3}{\mathbf{B}_2 + \mathbf{V}_2} \quad (3.11)$$

$$= A_{2\rightarrow 3}^{\text{LO}} \left( 1 - \Delta_2^1(m_Z^2, t_3) - \frac{\mathbf{V}_2}{\mathbf{B}_2} + \frac{\mathbf{V}_3}{\mathbf{B}_3} \right) + \mathcal{O}(\alpha_s^3), \quad (3.12)$$

---

<sup>2</sup>This very simple form assumes no mixing between different Born states at the 3-parton level. This is true for  $Z$  decays but not, e.g., for  $H \rightarrow Q\bar{Q}g$ . In that case, our procedure for treating mixing between different Born states would need to be applied. This is described in sec. 3.2.1.

<sup>3</sup>For the specific case of  $Z$  decay, the generic notation used here is somewhat overkill; the only explicit dependence on the 2-parton phase space,  $\hat{\Phi}_2(\Phi_3)$ , is via the total invariant mass,  $m_Z^2$ .

where the latter expansion reproduces the form of the matching equation proposed in ref. [32]. The form given in eq. (3.11) contains higher-order  $\alpha_s$  terms due to the choice of not expanding the  $B_2 + V_2$  terms in eq. (3.8). We return to the impact of such a choice in sec. 4.

In the context of NNLO matching to inclusive  $Z$  decays, it is this antenna function,  $A_{2\rightarrow 3}^{\text{NLO}}$ , that we shall seek to make fully explicit and implement in the VINCIA sector shower. The reason we called the matching equations provisional is that eqs. (3.11) and (3.12) are not yet complete and will require us to address a few more subtleties, including:

- Direct  $2 \mapsto 4$  branchings. This will be addressed immediately below.
- The calculation of  $V_3$  (and/or  $V_3^O$ ) explicitly, for the chosen jet algorithm that defines  $\hat{\Phi}_3(\Phi_4)$ , including how to arrange for the singularities between the real and virtual contributions to it to cancel analytically, and how to separate remaining terms into ones that can be done analytically (fast) and ones that require numerical treatment (slow). This will be the topic of sec. 3.1.
- The inclusion of  $g \rightarrow q\bar{q}$  splittings and interference between different Born processes, for example between  $Z \rightarrow u\bar{u} \oplus g \mapsto d\bar{d}$  and  $Z \rightarrow d\bar{d} \oplus g \mapsto u\bar{u}$ . These are addressed in sec. 3.2.
- Renormalisation-scale and -scheme choices. In the shower, the emission density is generally evaluated using a scale  $\mu_P^2 = \mathcal{O}(t_3) < \mu_M^2 = \mathcal{O}(m_Z^2)$ , and typically also employing the so-called CMW scheme [37]. This will likewise be relevant in constructing the explicit forms for the matching equations, and is addressed in sec. 3.3.
- Higher-order ambiguities. For example, eqs. (3.11) and (3.12) are equivalent up to terms of order  $\alpha_s^3$ ; the latter merely makes the modification to the LO antenna function at this order more explicit. In general, any fixed-order matching equation obviously leaves room for higher-order ambiguities, analogous to those between, e.g., MC@NLO and POWHEG-style approaches. We return to the explicit choices for these we make below, and in sec. 4.

First, it is important to note that the shower evolution will of course not stop at the 3-parton level but will continue afterwards, to generate 4-parton and higher-multiplicity states. For a general shower and a general observable, all of these paths would need to be followed and reclustered, to compute the specific observable at hand (which is precisely what a normal event-generator run does). However, since the sector shower generates the exact forward branching sequence that the ARCLUS algorithm reclusters, any configuration it does produce will be reclustered back to the starting configuration. So, as long as the subsequent shower evolution is unitary (i.e. does not change the weight of the event), the further evolution will not affect this particular observable at all, at any order. That is one reason why it is convenient to formulate the matching condition in terms of this particular observable, and why the sector shower is especially simple to work with.

Second, in a sector shower, there are parts of the 4-parton phase space (the “unordered” region) that cannot be reached by iterated  $2 \mapsto 3$  branchings. The solution implemented

in VINCIA is to allow direct  $2 \mapsto 4$  branchings [32, 38, 39] to populate those regions. It is straightforward to see that the tree-level matching conditions at the 4-parton level are:

$$A_{3 \mapsto 4}^{\text{LO}} = \frac{\mathbb{B}_4}{\mathbb{B}_3} + \mathcal{O}(\alpha_s^2), \quad (3.13)$$

$$A_{2 \mapsto 4}^{\text{LO}} = \frac{\mathbb{B}_4}{\mathbb{B}_2} + \mathcal{O}(\alpha_s^3), \quad (3.14)$$

where it is understood that the  $3 \mapsto 4$  matching condition is applied in the ordered part of phase space ( $t_3 > t_4$ ) while the  $2 \mapsto 4$  one is used in the unordered part. Note that these conditions also ensure that the product of iterated ME-corrected antenna functions in the ordered part reproduces the direct  $2 \mapsto 4$  one,

$$A_{2 \mapsto 3}^{\text{LO}} A_{3 \mapsto 4}^{\text{LO}} = A_{2 \mapsto 4}^{\text{LO}} + \mathcal{O}(\alpha_s^3). \quad (3.15)$$

Given that the 4-parton phase space is clearly sectorised into ordered and unordered regions, the NLO 3-jet rate in the sector shower must also incorporate the direct  $2 \mapsto 4$  branchings, namely for those configurations which cluster back to the 3-parton phase-space point  $\Phi_3 = \hat{\Phi}_3(\Phi_4)$ . The full expression for the differential shower rate then becomes

$$\begin{aligned} \frac{m_Z}{8\pi^4} \frac{d^5\Gamma}{d\Phi_3} = & (\mathbb{B}_2 + \mathbb{V}_2 + \mathbb{W}_2) \left[ \Delta_2(m_Z^2, t_3) A_{2 \mapsto 3} \right. \\ & \left. + \int_{t_3 < t_4} d\Phi_4 \Delta_2(m_Z^2, t_4) A_{2 \mapsto 4} \delta^{(5)}(\Phi_3 - \hat{\Phi}_3(\Phi_4)) \right], \end{aligned} \quad (3.16)$$

where the restriction  $t_3 < t_4$  comes from the fact that the direct  $2 \mapsto 4$  branchers only populate the unordered region. For the  $2 \mapsto 4$  emission density,  $A_{2 \mapsto 4}$ , the 4-parton tree-level matching condition eq. (3.14) applies. For double-gluon emissions at leading colour in  $Z$  decay, this makes the  $2 \mapsto 4$  emission density identical to the GGG antenna function  $A_4^0$  [36] (modulo the colour and coupling factor). Equivalent functions exist for the  $g \rightarrow q\bar{q}$  contributions but we defer a detailed discussion of them to later sections.

The Sudakov factor that represents the no-branching probability of the shower evolution from the “pre-Born” 2-parton state likewise includes both  $2 \mapsto 3$  and  $2 \mapsto 4$  contributions:

$$\Delta_2 = \Delta_{2 \mapsto 4} \Delta_{2 \mapsto 3}. \quad (3.17)$$

In the context of NLO matching, we are only interested in the  $\mathcal{O}(\alpha_s)$  expansion of this expression. The  $2 \mapsto 4$  Sudakov factor only generates terms starting from  $\mathcal{O}(\alpha_s^2)$  and hence does not contribute at  $\mathcal{O}(\alpha_s)$ . The expansion of the  $2 \mapsto 3$  Sudakov factor is given by eq. (3.9), which we rewrite using antenna phase-space factorisation,

$$\Delta_2^1 = \Delta_{2 \mapsto 3}^1(m_Z^2, t_3) = - \int_{t_3}^{m_Z^2} d\Phi'_{+1} \frac{\mathbb{B}'_3}{\mathbb{B}_2}, \quad (3.18)$$



where we have used primes to distinguish the 3-parton phase space that is being integrated over from the (fixed) 3-parton configuration that defines  $t_3$  (unprimed). That is,  $\mathbb{B}'_3$  depends on the 2-parton and antenna phase spaces,

$$\mathbb{B}'_3 \equiv \mathbb{B}_3(\Phi'_3) = \mathbb{B}_3(\Phi_2, \Phi'_{+1}), \quad (3.19)$$

$$d\Phi_{+1} = \frac{1}{16\pi^2 m_Z^2} ds_{qg} ds_{g\bar{q}} \frac{d\varphi}{2\pi}. \quad (3.20)$$

We emphasise that the (massless) antenna phase space is the standard one used, e.g., in refs. [36, 40].

Expanding eq. (3.16) to  $\mathcal{O}(\alpha_s^2)$  therefore yields the same matching equation for the NLO antenna function as in eq. (3.8), with  $\mathbb{V}_3$  replaced by  $\mathbb{V}_3^{\text{O}}$ ,

$$(\mathbb{B}_2 + \mathbb{V}_2) (1 + \Delta_2^1(m_Z^2, t_3)) A_{2 \rightarrow 3}^{\text{NLO}} = \mathbb{B}_3 + \mathbb{V}_3^{\text{O}} + \mathcal{O}(\alpha_s^3). \quad (3.21)$$

Solving this for  $A_{2 \rightarrow 3}^{\text{NLO}}$  yields [38, 39]

$$A_{2 \rightarrow 3}^{\text{NLO}} = \frac{\mathbb{B}_3 (1 - \Delta_2^1(m_Z^2, t_3)) + \mathbb{V}_3^{\text{O}}}{\mathbb{B}_2 + \mathbb{V}_2} + \mathcal{O}(\alpha_s^3), \quad (3.22)$$

which is the form we shall use. Up to higher-order ambiguities (which we return to in sec. 4) and term(s) translating between different renormalisation-scheme and -scale choices, which are simple to add [38], this equation defines the NLO 3-jet correction coefficient for the NNLO matched shower.

The integral in eq. (3.18), which we sometimes refer to as the ‘‘Sudakov on top’’ — since it originates from the one-loop expansion of the  $2 \mapsto 3$  shower evolution — is [38]:

$$-\int_{t_3}^{m_Z^2} d\Phi'_{+1} \frac{|M_3^{0'}|^2}{|M_2^0|^2} = -\frac{\alpha_s C_F}{2\pi} \left[ \ln^2 \tau_3 + 2\text{Li}_2(1 - x_+) - 2\text{Li}_2(x_+) + 3 \ln \tau_3 \right. \\ \left. + 6(\sqrt{1 - 4\tau_3} - \ln x_+) - 2 \ln \tau_3 \ln x_+ \right], \quad (3.23)$$

with

$$\tau_3 = \frac{t_3}{m_Z^2}, \quad x_+(\tau_3) = \frac{1 + \sqrt{1 - 4\tau_3}}{2} \quad \left( \rightarrow 1 \text{ for } \tau_3 \rightarrow 0 \right). \quad (3.24)$$

For reference, we note that the IR limit of eq. (3.23) as  $\tau_3 \rightarrow 0$  is:

$$-\frac{\alpha_s C_F}{2\pi} \left[ \ln^2 \tau_3 + 3 \ln \tau_3 - \frac{\pi^2}{3} + 6 \right]. \quad (3.25)$$

If the decaying particle is a scalar instead of a vector, then the 3-parton matrix element includes an additional non-singular term  $\alpha_s C_F / (\pi m_H^2)$ , which implies a further term to be added to eq. (3.23) in the case of Higgs decay,

$$-\frac{\alpha_s C_F}{2\pi} \left[ \sqrt{1 - 4\tau_3} + 2\tau_3 (\ln(x_+) - \ln(1 - x_+)) \right] \quad (3.26)$$

whose IR limit is  $-\alpha_s C_F/(2\pi)$ .

Eqs. (2.9) and (2.11) (for  $V_3$  and  $V_3^O$  respectively) each contain two terms. We shall assume that the first one, containing the one-loop amplitude, is dealt with externally, analytically and/or by a numerical one-loop provider, using dimensional regularisation and cast in a way that makes its pole structure and finite remainders explicit. Our main remaining task is then to bring the second term, representing the integral over singly-clustered 4-parton configurations, to an equivalent form — with explicit poles that cancel those of the first term, and (numerically stable) finite remainders.

We focus on the integral over 4-parton states that cluster back to the 3-parton state at hand,

$$I_{3\leftarrow 4}(\Phi_3) = \int_{t_3 > t_4} d\Phi_4 \mathbf{B}_4 \delta^{(5)}\left(\Phi_3 - \hat{\Phi}_3(\Phi_4)\right), \quad (3.27)$$

where we reiterate that the restriction to ordered clusterings here,  $t_3 > t_4$ , came from matching the fixed-order integral (which included all of phase space) to a shower that includes direct  $\mathcal{O}(\alpha_s^2)$   $2 \mapsto 4$  branchings in the unordered region.<sup>4</sup>

We start by setting up the notation following the conventions of ref. [36]. The four-parton final state ( $qgg\bar{q}$ ) is labelled as follows

$$(1_q, 3_g, 4_g, 2_{\bar{q}}), \quad (3.28)$$

while the inverse mapping  $3 \leftarrow 4$  leads to a  $qg\bar{q}$  state denoted as follows

$$(\hat{1}_q, \hat{3}_g, \hat{2}_{\bar{q}}). \quad (3.29)$$

The fact that we are using a deterministic sequential-clustering jet algorithm divides the phase space up into sectors according to the gluon that has the lowest value of the jet resolution measure. At the colour-ordered level, there are then two sectors, which we label  $A$  and  $B$ , corresponding to clusterings of gluons 3 and 4 respectively. Thus,

$$I_{3\leftarrow 4}(\Phi_3) = \mathbf{B}_2 \int_{\hat{t}_3 > t_{4A}} d\Phi_{+1}^A \Theta(t_{4B} - t_{4A}) A_{2\rightarrow 4}^{\text{LO}} + (A \leftrightarrow B), \quad (3.30)$$

again with the standard massless antenna phase space (in  $4 - 2\epsilon$  dimensions)

$$d\Phi_{+1}^A = \left(\frac{4\pi\mu^2}{\hat{s}_{qg}}\right)^\epsilon \frac{1}{\Gamma(1-\epsilon)} \frac{\hat{s}_{qg}}{16\pi^2} dy_{13} dy_{34} dy_{14} (y_{13} y_{34} y_{14})^{-\epsilon} \frac{d\Omega_{2-2\epsilon}}{\Omega_{2-2\epsilon}} \quad (3.31)$$

$$\stackrel{\epsilon \rightarrow 0}{=} \frac{\hat{s}_{qg}}{16\pi^2} dy_{13} dy_{34} \frac{d\varphi}{2\pi}, \quad (3.32)$$

---

<sup>4</sup>Note that exactly the same matching equation would have resulted, with the same form of eq. (3.27), should we have used a modified form of the jet algorithm in which direct  $4 \mapsto 2$  clusterings would be allowed.

where the scaled invariants are  $y_{ij} = s_{ij}/\hat{s}_{qg}$  (with  $y_{13} + y_{14} + y_{34} = 1$ ), and the three- and four-parton resolution scales defined by our jet-clustering measure are

$$\hat{t}_3 = \frac{\hat{s}_{qg}\hat{s}_{g\bar{q}}}{m_Z^2}, \quad (3.33)$$

$$t_{4A} = \frac{s_{13}s_{34}}{s_{134}}, \quad (3.34)$$

$$t_{4B} = \frac{s_{24}s_{34}}{s_{234}}. \quad (3.35)$$

The fact that the step functions in eq. (3.30) involve the invariants  $s_{24}$  and  $s_{234}$ , which go outside of the local  $2 \mapsto 3$   $d\Phi_{+1}^A$  and are only determined by the explicit kinematic map (i.e., the inverse of the clustering map), is the main challenge in working with these integrals. We have considered two possible paths to dealing with this, one based on global antenna subtraction, and one based on a new sector antenna subtraction.

In both cases, the ultimate goal is to construct a numerical contribution which is stable and quick to evaluate, while achieving pole cancellation analytically. The formulations presented here are quite general and work for any antenna function that appears in the integrand, given properly constructed subtraction terms in  $4 - 2\epsilon$  dimensions.

### 3.1 NLO 3-jet matching with sector subtraction

Here, we present a computation of the leading-colour (LC) NLO 3-jet matching coefficient, in which the subtraction term is also sectorised. An alternative approach, derived via global antenna subtraction, is given in appendix C.

Without loss of generality, we focus on the  $A$  sector and then later show how to bootstrap the result for the  $B$  sector, namely we wish to compute

$$I_{3\leftarrow 4}^A = \mathbb{B}_3 \frac{g^2 N_C}{A_3^0(\hat{1}_q, \hat{3}_g, \hat{2}_{\bar{q}})} \int_{\hat{t}_3 > t_{4A}} d\Phi_{+1}^A \Theta(t_{4B} - t_{4A}) A_4^0, \quad (3.36)$$

where we have now made colour and coupling factors explicit, multiplying the GGG  $A_3^0$  and  $A_4^0$  antenna functions for  $Z$  decay [36]. The three- and four-parton resolution scales,  $t_i$ , and the antenna phase space are defined in eqs. (3.31) – (3.35).

To understand how to best perform the computation, it is helpful to investigate the sector constraint in eq. (3.36) upon implementing an explicit kinematic map. We shall demonstrate the important features of the sector constraint using a generic antenna map, e.g. for a  $qg$  antenna,

$$p_1 = a_1 \hat{p}_q + b_1 \hat{p}_g + c p_\perp, \quad (3.37)$$

$$p_3 = a_3 \hat{p}_q + b_3 \hat{p}_g - p_\perp, \quad (3.38)$$

$$p_4 = a_4 \hat{p}_q + b_4 \hat{p}_g + (1 - c) p_\perp, \quad (3.39)$$

where the variable  $p_\perp$  is the standard transverse momentum in the Sudakov parametrisation (it is spacelike and orthogonal to  $\hat{p}_q$  and  $\hat{p}_g$ ). We note that it is simply a parametric variable which should not be confused with the shower evolution variable, which we denote

by  $t$ . The quantities  $a_i$ ,  $b_i$  and  $c$  encode the explicit kinematic map and are a function of  $(y_{13}, y_{34})$ . We emphasise that this representation is general for local antenna kinematics; in particular all of the maps so far implemented in VINCIA (i.e., the so-called ARIADNE [41], Kosower [42], and dipole [43] maps) correspond to different functional forms of  $c(y_{13}, y_{34})$ . Nevertheless, the latter has to satisfy the following conditions in the quark-gluon and gluon-gluon collinear limits,

$$\lim_{y_{13} \rightarrow 0} c(y_{13}, y_{34}) = 1, \quad \lim_{y_{34} \rightarrow 0} c(y_{13}, y_{34}) = 0. \quad (3.40)$$

From energy-momentum conservation and on-shell conditions we also have

$$a_1 + a_3 + a_4 = b_1 + b_3 + b_4 = 1, \quad -p_\perp^2 = p_t^2 = a_3 b_3 \hat{s}_{qg}. \quad (3.41)$$

It is clear that the sector constraint in eq. (3.36) explicitly depends on the anti-quark momentum  $p_2$ . For local antenna kinematics,  $p_2$  does not participate in the  $4 \mapsto \hat{3}$  clustering for sector  $A$ , i.e.,  $p_2 = \hat{p}_{\bar{q}}$ . To proceed, we introduce a Sudakov decomposition of  $p_2$  in terms of the Born+1 momenta  $(\hat{p}_q, \hat{p}_g)$ :

$$p_2 = a_2 \hat{p}_q + b_2 \hat{p}_g + p_{\perp 2}, \quad (3.42)$$

and it is straightforward (by on-shellness) to derive expressions for the Sudakov coefficients in terms of Born+1 invariants

$$a_2 = \frac{\hat{y}_{q\bar{q}}}{\hat{y}_{qg}}, \quad b_2 = \frac{\hat{y}_{g\bar{q}}}{\hat{y}_{qg}}, \quad p_{t2}^2 = a_2 b_2 \hat{s}_{qg}, \quad (3.43)$$

with  $\hat{y}_{ij} = \hat{s}_{ij}/m_Z^2$ .

From this last step, we can glean the important features of the sector constraint, and we do so by inspecting its azimuthal dependence. The azimuthal angle,  $\varphi$ , in the antenna phase space, eq. (3.32), can be chosen to be the relative angle between the 2-dimensional transverse vectors  $p_\perp$  and  $p_{\perp 2}$ . Therefore, in terms of the antenna phase-space variables the sector constraint can be rearranged as follows

$$\Theta(t_{4B} - t_{4A}) = \Theta(f(y_{13}, y_{34}; \hat{y}_{qg}, \hat{y}_{g\bar{q}}, \hat{y}_{q\bar{q}}) - \cos \varphi), \quad (3.44)$$

where the function  $f$  depends explicitly on the specific map, as defined through the choice of  $c(y_{13}, y_{34})$ . We obtain

$$f(y_{13}, y_{34}; \hat{y}_{qg}, \hat{y}_{g\bar{q}}, \hat{y}_{q\bar{q}}) = \frac{(1 - y_{13})(a_2 b_4 + a_4 b_2) - y_{13}(a_2 b_3 + b_2 a_3) - y_{13} y_{34}}{2 \sqrt{\frac{\hat{y}_{q\bar{q}} \hat{y}_{g\bar{q}}}{\hat{y}_{qg}^2}} (1 - (1 - y_{13})c) \sqrt{a_3 b_3}}. \quad (3.45)$$

Thus the sector constraint boils down to two distinct regions in  $\varphi$ : one in which there is no constraint on  $\varphi$ , corresponding to  $f > 1$ , and one in which the  $\varphi$  range is bounded, in the region where  $|f| < 1$ :

$$\Theta(t_{4B} - t_{4A}) = \Theta(f > 1) \Theta(0 < \varphi < \pi) + \Theta(-1 < f < 1) \Theta(\varphi < \cos^{-1}(f)). \quad (3.46)$$

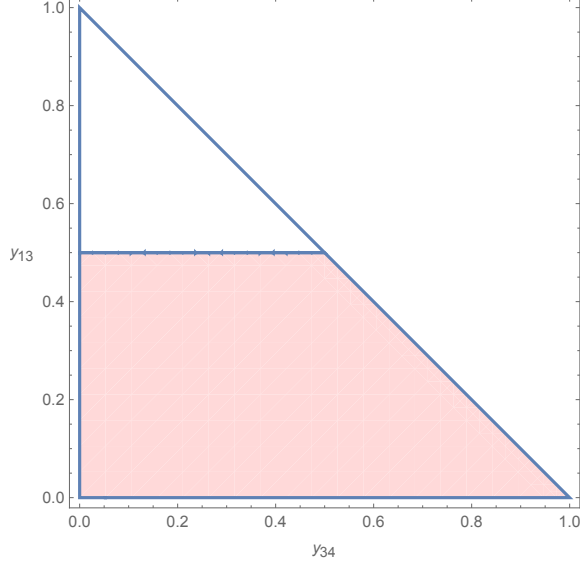


**Figure 1.** The Dalitz plane for the evaluation of eq. (3.36). All singularities persist in the red-filled polygon, while the empty triangle is singularity-free by virtue of the sector constraint.

To study the behaviour of  $f$  in the singular limits, we utilise the explicit expressions of the Sudakov coefficients from ref. [9] and eq. (3.40). In the limit  $y_{13} \rightarrow 0$ , we obtain

$$\lim_{y_{13} \rightarrow 0} f(y_{13}, y_{34}; \hat{y}_{qg}, \hat{y}_{g\bar{q}}, \hat{y}_{q\bar{q}}) = +\infty, \quad (3.47)$$

and so, as  $y_{13} \rightarrow 0$ , the  $\varphi$ -integral is unconstrained as per eq. (3.46). The limit  $y_{34} \rightarrow 0$  is more interesting. At fixed  $y_{13}$ , we have two cases:

$$\lim_{y_{34} \rightarrow 0} f(y_{13}, y_{34}; \hat{y}_{qg}, \hat{y}_{g\bar{q}}, \hat{y}_{q\bar{q}}) = \begin{cases} +\infty, & \text{if } y_{13} < \frac{1}{2} \\ -\infty, & \text{if } y_{13} > \frac{1}{2}. \end{cases} \quad (3.48)$$

Therefore, from eq. (3.46) we conclude that the region  $y_{13} > \frac{1}{2}$  is completely regular (i.e., free of singularities) because the sector step function in this limit vanishes. In other words, the sector constraint shields the singularity  $y_{34} \rightarrow 0$  in the region  $y_{13} > 1/2$  of the Dalitz space. This is illustrated in fig. 1.

Crucially, this analysis holds for any local kinematic map, because the singular limits of both the Sudakov coefficients and the function  $c$  are independent of the specific map. Moreover, we can construct a subtraction term that is only nonzero for  $y_{13} < \frac{1}{2}$ , i.e. in the red region of fig. 1.

A suitable subtraction term must incorporate the correct singular limits of  $A_4^0$  *only* in the red region. In particular the subtraction term must reproduce the full  $g \rightarrow gg$  splitting function in the  $3||4$  limit. With this understanding we introduce the following function in the 4-parton phase space<sup>5</sup>

$$D_3^{s0}(1_q, 3_g, 4_g) = \frac{1}{s_{134}} \left( \frac{2y_{14}}{y_{13}y_{34}} + \frac{2y_{13}}{(1-y_{13})y_{34}} + (1-\epsilon)\frac{y_{34}}{y_{13}} + \frac{2y_{13}y_{14}}{y_{34}} \right), \quad (3.49)$$

<sup>5</sup>We note that improved antenna subtraction terms have also been discussed in ref. [44].

where  $y_{14} = 1 - y_{13} - y_{34}$ . Indeed this subtraction function has all the correct limits:

$$\lim_{y_{13} \rightarrow 0} D_3^{\text{s}0} = \frac{1}{y_{13}} p_{gq}(z, \epsilon), \quad \lim_{y_{34} \rightarrow 0} D_3^{\text{s}0} = \frac{1}{y_{34}} p_{gg}(z, \epsilon), \quad (3.50)$$

where  $z$  is the energy (light-cone momentum) fraction carried by  $3_g$  and the DGLAP splitting functions are

$$p_{gq}(z, \epsilon) = \frac{1 + (1 - z)^2}{z} - \epsilon z, \quad p_{gg}(z, \epsilon) = 2 \frac{(1 - z(1 - z))^2}{z(1 - z)}. \quad (3.51)$$

We can now utilise the subtraction function  $D_3^{\text{s}0}$  in eq. (3.49) to rewrite the core eq. (3.36) as:

$$\begin{aligned} I_{3 \leftrightarrow 4}^A = & \mathbf{B}_3 \frac{g^2 N_C}{A_3^0(\hat{1}_q, \hat{3}_g, \hat{2}_{\bar{q}})} \int_{\hat{t}_3 > t_{4A}} d\Phi_{+1}^A \Theta(t_{4B} - t_{4A}) \left[ A_4^0 - A_3^0(\hat{1}_q, \hat{3}_g, \hat{2}_{\bar{q}}) D_3^{\text{s}0} \Theta\left(y_{13} < \frac{1}{2}\right) \right] \\ & + \mathbf{B}_3 g^2 N_C \int_{\hat{t}_3 > t_{4A}} d\Phi_{+1}^A \Theta(t_{4B} - t_{4A}) \left[ D_3^{\text{s}0} \Theta\left(y_{13} < \frac{1}{2}\right) \right]. \end{aligned} \quad (3.52)$$

The first line is free of singularities and can be integrated in 4 dimensions via a MC procedure. The integral of the subtraction term is a bit more complicated than usual, due to the presence of the sector constraint.

To confirm that we have a proper subtraction term, we integrate the second line of eq. (3.52) over the antenna phase space, and check that we recover the pole structure of the real-virtual term. This gives<sup>6</sup>

$$\begin{aligned} (8\pi^2) \int_{\hat{t}_3 > t_{4A}} d\Phi_{+1}^A D_3^{\text{s}0} \Theta\left(y_{13} < \frac{1}{2}\right) \\ = \left(\frac{\mu_R^2}{m_Z^2}\right)^\epsilon \frac{\hat{y}_{q\bar{q}}^{-\epsilon}}{2} \left(\frac{2}{\epsilon^2} + \frac{10}{3\epsilon} + \frac{453}{48} - \pi^2 - \frac{\ln 2}{3}\right) - \mathcal{F}(\hat{y}_{q\bar{q}}), \end{aligned} \quad (3.53)$$

where  $\mathcal{F}(\hat{y}_{q\bar{q}})$  is a finite function which is given in appendix A.

This is indeed the correct pole structure required to cancel out the poles in the real-virtual term, see appendix B. The canonical GGG sub-antenna, i.e.  $d_3^A$ , gives *half* of the  $g \rightarrow gg$  splitting function in the  $y_{34} \rightarrow 0$  limit. In this case, integrating over the whole Dalitz triangle results in the correct single pole, i.e.  $10/3\epsilon$ . With our new subtraction term given in eq. (3.49), although we recover the full  $p_{gg}$  in the  $y_{34} \rightarrow 0$  collinear limit, we still obtain the correct single pole because we restrict the integration domain to  $y_{13} < \frac{1}{2}$ .

However, the second line of eq. (3.52) requires that we implement the full sector constraint,  $\Theta(t_{4B} - t_{4A})$ . This does not present any difficulty, because as we see in eq. (3.53) all the poles are correctly reproduced. Therefore, in addition to eq. (3.53) we have the following left-over term, which is integrable in four dimensions:

$$\int_{\hat{t}_3 > t_{4A}} d\Phi_{+1}^A D_3^{\text{s}0} \Theta\left(y_{13} < \frac{1}{2}\right) \left[ \Theta(t_{4B} - t_{4A}) - 1 \right]. \quad (3.54)$$

<sup>6</sup>To obtain this expression, charge renormalisation has been effected, i.e.  $\alpha_s(\mu_R) \rightarrow \alpha_s(\mu_R)(4\pi)^{-\epsilon} e^{\epsilon\gamma_E}$ .

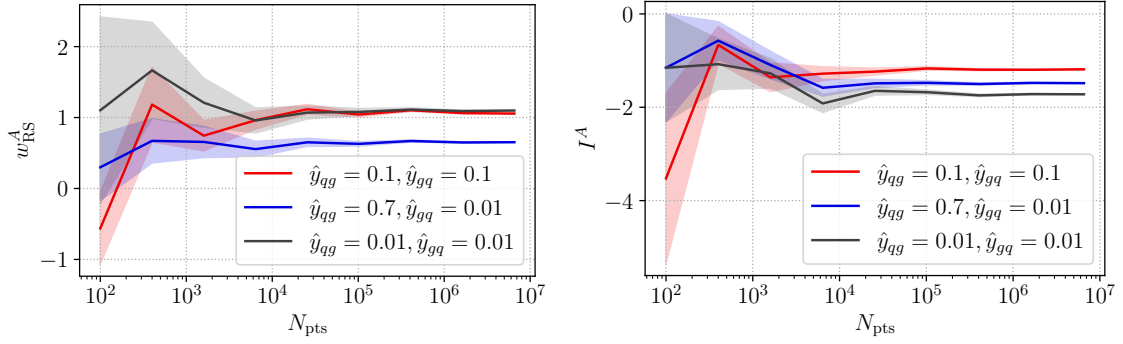


**Figure 2.** The numerical evaluation of the  $w_{\text{RS}}^A$  (left) and  $\mathcal{I}^A$  (right) contributions for various Born+1 configurations, as a function of the number of points used in the MC evaluation.

### 3.1.1 Summary of matching by sector subtraction

We are in a position to collate all the pieces to rewrite eq. (3.36), which gives

$$\begin{aligned}
I_{3\leftarrow 4}^A &= \text{B}_3 \left( \frac{\alpha_s N_C}{2\pi} \right) \left( \frac{\mu_R^2}{m_Z^2} \right)^\epsilon \left( \frac{\hat{y}_{qg}^{-\epsilon}}{2} \left( \frac{2}{\epsilon^2} + \frac{10}{3\epsilon} + \frac{453}{48} - \pi^2 - \frac{\ln 2}{3} \right) - \mathcal{F}(\hat{y}_{g\bar{q}}) \right) \\
&+ \text{B}_3 \left( \frac{\alpha_s N_C}{2\pi} \right) (w_{\text{RS}}^A(\hat{y}_{qg}, \hat{y}_{g\bar{q}}) + \mathcal{I}^A(\hat{y}_{qg}, \hat{y}_{g\bar{q}})) , \tag{3.55}
\end{aligned}$$

where we defined:

$$w_{\text{RS}}^A = \frac{8\pi^2}{A_3^0(\hat{1}_q, \hat{3}_g, \hat{2}_{\bar{q}})} \int_{\hat{t}_3 > t_{4A}} d\Phi_{+1}^A \Theta(t_{4B} - t_{4A}) \left[ A_4^0 - A_3^0(\hat{1}_q, \hat{3}_g, \hat{2}_{\bar{q}}) D_3^{s0} \Theta\left(y_{13} < \frac{1}{2}\right) \right] , \tag{3.56}$$

and

$$\mathcal{I}^A = 8\pi^2 \int_{\hat{t}_3 > t_{4A}} d\Phi_{+1}^A D_3^{s0} \Theta\left(y_{13} < \frac{1}{2}\right) \left[ \Theta(t_{4B} - t_{4A}) - 1 \right] . \tag{3.57}$$

The integrals in eqs. (3.56) and (3.57) are computed numerically and shown in fig. 2 for various Born+1 configurations. We notice good convergence with increasing the number of sampling points. In the MC evaluation of fig. 2 we use the sampling of the antenna phase space  $d\Phi_{+1}$  described in ref. [45].

### 3.1.2 Bootstrapping the $B$ sector

To obtain the final result as given by eq. (3.30), we must include the contribution from the  $B$  sector, i.e. the term  $A \leftrightarrow B$ . This does not require any further computation, as the result can be obtained from the  $A$  sector by the simple swap

$$\hat{y}_{qg} \rightarrow \hat{y}_{g\bar{q}}, \quad \hat{y}_{g\bar{q}} \rightarrow \hat{y}_{qg} , \tag{3.58}$$

and thus

$$I_{3\leftarrow 4}^B(\hat{y}_{qg}, \hat{y}_{g\bar{q}}) = I_{3\leftarrow 4}^A(\hat{y}_{g\bar{q}}, \hat{y}_{qg}) .$$

The numerical contribution from both sectors,

$$\left(\frac{\alpha_s N_C}{2\pi}\right) (w_{\text{RS}}^A + \mathcal{I}^A + w_{\text{RS}}^B + \mathcal{I}^B), \quad (3.59)$$

is shown in fig. 3 as a function of the Born+1 variables.

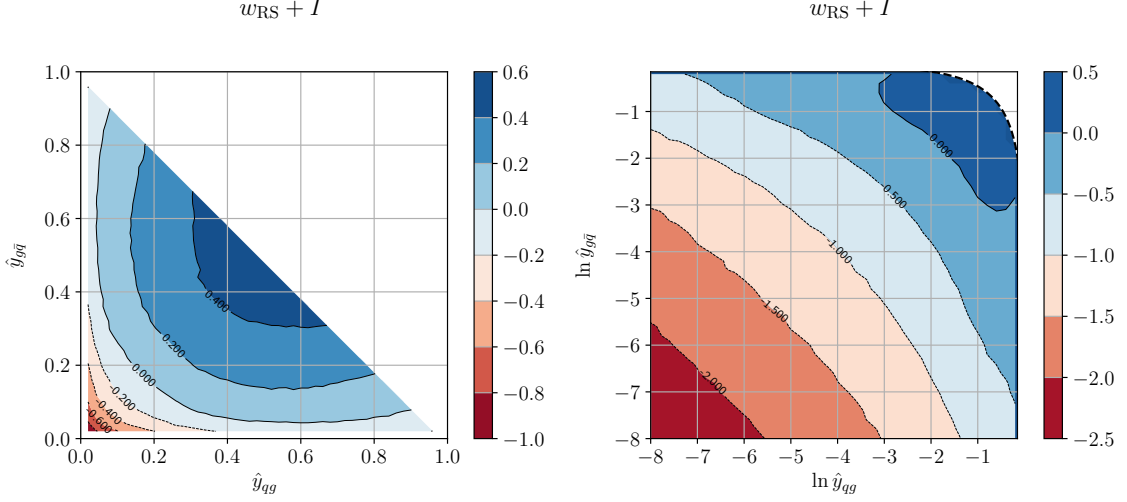


**Figure 3.** The numerical contribution from eq. (3.59) as a function of  $(\hat{y}_{qg}, \hat{y}_{g\bar{q}})$  (left) and in logarithmic space (right).

### 3.1.3 The $v^{\text{NLO}}$ factor

Adding in the virtual corrections, which are given in appendix B, we are now ready to write down the final result of eq. (2.11),

$$V_3^{\text{O}} = B_3 \times v^{\text{NLO}}(\hat{y}_{qg}, \hat{y}_{g\bar{q}}), \quad (3.60)$$

where the  $N_C$  piece is given by

$$v_{N_C}^{\text{NLO}} = \left(\frac{\alpha_s N_C}{2\pi}\right) (w_{\text{RS}}^A + \mathcal{I}^A + w_{\text{RS}}^B + \mathcal{I}^B + w_\gamma), \quad (3.61)$$

and  $w_\gamma$  is the finite analytic function that results from combining virtual corrections and the integrated subtraction term, i.e. the first line of eq. (3.55) and its equivalent for sector  $B$ . The expression of the latter is somewhat lengthy and thus we do not report it here. Nevertheless, it is instructive to extract the logarithmic structure present in the analytic function  $w_\gamma$  in all unresolved limits of the Born+1 state. Using the notation of eq. (3.24), we obtain ( $\tau_3 = \hat{y}_{qg}\hat{y}_{g\bar{q}}$ )

$$\lim_{\tau_3 \rightarrow 0} w_\gamma \rightarrow -\frac{1}{2} \ln^2 \tau_3 - \frac{10}{3} \ln \tau_3 - \frac{11 \ln 2}{6} + \frac{\pi^2}{3} - \frac{31}{72}. \quad (3.62)$$



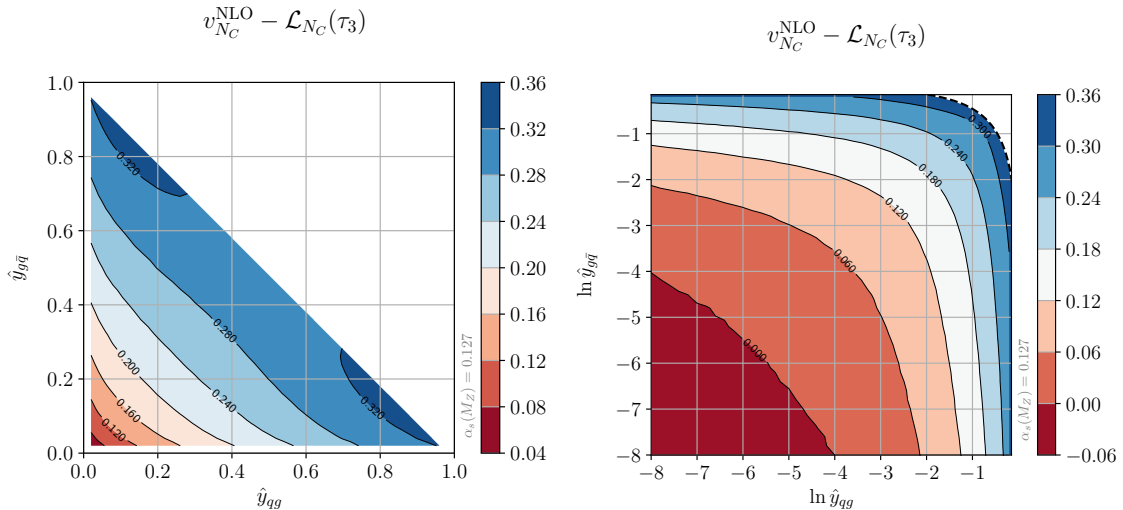


**Figure 4.** The contribution  $v_{NC}^{\text{NLO}}$  as a function of  $(\hat{y}_{qg}, \hat{y}_{g\bar{q}})$  (left) and in logarithmic space (right). Here, we subtract the expected logarithmic terms  $\mathcal{L}(\tau_3) = -\frac{1}{2} \ln^2 \tau_3 - \frac{10}{3} \ln \tau_3$ , with  $\tau_3 = \hat{y}_{qg} \hat{y}_{g\bar{q}}$  in eq. (3.62) from the full correction.

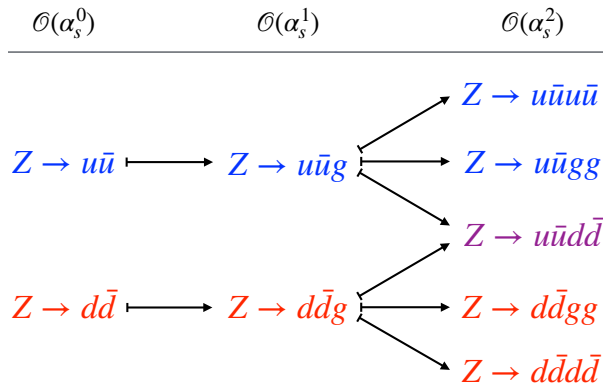


**Figure 5.** Illustration of shower histories starting from  $Z \rightarrow u\bar{u}$  (blue) and  $Z \rightarrow d\bar{d}$  (red). Both histories are allowed to contribute to the *same* phase-space points for  $Z \rightarrow u\bar{u}d\bar{d}$  (purple).

### 3.2 The $N_F$ piece

For the gluon-splitting contributions to the 4-parton integrals, there are two further subtleties:

1. Interference between shower histories that originate from different Born processes: e.g.,  $Z \rightarrow u\bar{u}d\bar{d}$  receives contributions from both  $Z \rightarrow u\bar{u}g \otimes g \rightarrow d\bar{d}$  and from  $Z \rightarrow d\bar{d}g \otimes g \rightarrow u\bar{u}$  shower histories. This is illustrated in fig. 5. Each of these effectively represents an integration channel with a specific singularity structure. After matching, these need to sum up to the full four-parton squared matrix element including interference terms, point by point in phase space and with the correct combinations of  $q\bar{q}Z$  couplings. We note that, in fixed-order contexts, this subtlety can often be neglected, as fermion antisymmetry implies that the interference cancels in

observables that are not sensitive to charge signs. But this would not be true of the subsequent shower evolution, and moreover we shall want the matched MC evolution algorithm to be NNLO correct not only for charge-blind observables but also for charge-sensitive ones.

2. The sector resolution variable we choose for  $g \rightarrow q\bar{q}$  splittings has to be slightly different from the evolution variable  $t_{[j]/ik}$  that was used in the gluon-emission case [28, 31]. (Otherwise neighbouring collinear  $gq$  singularities would be undercounted.)

We shall now address each of these subtleties in turn, before presenting the full form of the  $N_F$  part of  $V_3$ .

### 3.2.1 Multiple interfering Born states

Consider, e.g.,  $Z \rightarrow u\bar{u}d\bar{d}$ . In a global antenna shower, the total rate in each  $u\bar{u}d\bar{d}$  phase-space point would result from a sum over four different histories:

1.  $u\bar{u} \mapsto (ug \mapsto u\bar{d}d)\bar{u}$ ,
2.  $u\bar{u} \mapsto u(g\bar{u} \mapsto \bar{d}d\bar{u})$ ,
3.  $d\bar{d} \mapsto (dg \mapsto d\bar{u}u)\bar{d}$ ,
4.  $d\bar{d} \mapsto d(g\bar{d} \mapsto \bar{u}u\bar{d})$ .

In a sector shower, one has a choice: sectorise across all four of these histories so that only *one* of them is allowed to contribute to each phase-space point, or sectorise only across subsets that share the same Born configuration. For hadronic  $Z$ -decays, this choice is not critical since the Born-level couplings to different quark flavours have similar orders of magnitude. But to preempt cases like  $H \rightarrow q\bar{q}$  for which the Born-level couplings can be vastly different, we opt for the latter, namely to sectorise only between shower histories that share the same Born-level configurations. This is in line with what is already done in VINCIA’s sector merging [46].

This implies that, during the shower evolution off a  $u\bar{u}$  Born state, only sectors that represent clusterings back to configurations with at least one  $u\bar{u}$  pair will be taken into consideration (for the purpose of sectoring), while sector conditions are not checked for clusterings that represent other Born states. Similarly for the shower evolution off  $d\bar{d}$  states, no sector conditions are imposed for clusterings that correspond to  $u\bar{u}$  Born states (and analogously for higher numbers of flavours). In this sense, partons that are present at the Born level are also considered “hard” or “unclusterable”.

Since there is no sectoring between different Born states, the sector-shower rate for parton states that can be reached from multiple Born states will thus contain a sum of terms, one for each distinct Born state. Each such term mimics the leading singularity structure of a specific subset of squared amplitudes — involving that particular set of Born couplings.<sup>7</sup>

---

<sup>7</sup>Of course the full matrix elements will include interferences between the different Born processes. In the context of matching, it is important to note that it is the *sum* over sector-shower histories that we shall seek to match to the full result. Below, we introduce a few extra notational devices to hopefully make it clear when and where interferences are included.

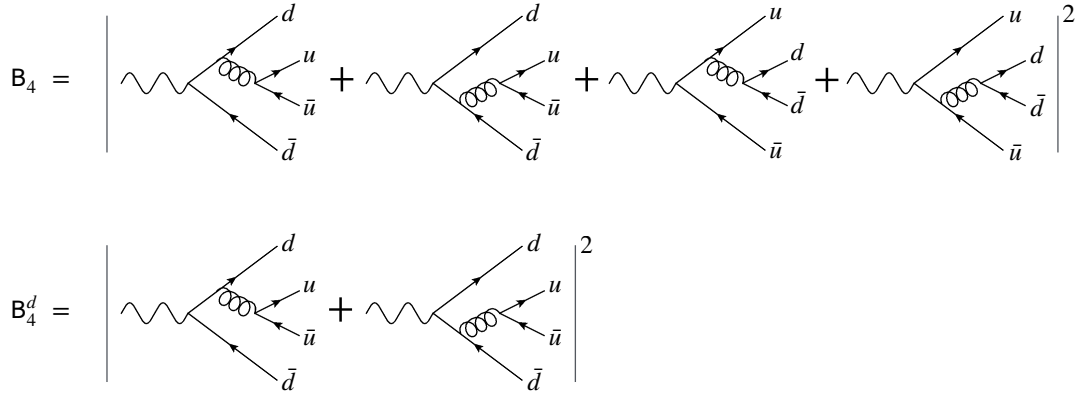


**Figure 6.** Illustration of multiple Born histories, for a  $Z \rightarrow u\bar{u}d\bar{d}$  final state. *Top:* the full squared matrix element, denoted  $B_4$ , contains an interference term between diagrams with  $\bar{d}dZ$  couplings and diagrams with  $\bar{u}uZ$  ones. *Bottom:* in the coefficient denoted  $B_4^d$ , only diagrams with Born-level  $\bar{d}dZ$  coupling are included.

Continuing with the example of the 4-parton state  $Z \rightarrow u\bar{u}d\bar{d}$ , we need the sum of the two contributions,

$$Z \rightarrow u\bar{u}g \otimes g \mapsto d\bar{d} \quad + \quad Z \rightarrow d\bar{d}g \otimes g \mapsto u\bar{u}, \quad (3.63)$$

to reproduce the full matrix element. Fig. 6 illustrates the full squared matrix element for the 4-parton state (top row), as well as the contribution proportional to a single  $Z$  coupling (bottom row), which we will use in constructing the interference-correction factor below.

For the path  $Z \rightarrow d\bar{d} \oplus g \mapsto u\bar{u}$ , we generalise eqs. (3.13) & (3.14) to include an interference-factor,  $k_I$ :

$$A_{3 \rightarrow 4}^{\text{LO}} = k_I^{du} \frac{B_4^d}{B_3^d} + \mathcal{O}(\alpha_s^2), \quad (3.64)$$

$$A_{2 \rightarrow 4}^{\text{LO}} = k_I^{du} \frac{B_4^d}{B_2^d} + \mathcal{O}(\alpha_s^3), \quad (3.65)$$

where  $B_{2,3}^q$  are the Born-level squared matrix elements for  $Z \rightarrow q\bar{q}$  and  $Z \rightarrow q\bar{q}g$  respectively, and

$$B_4^d = B_2^d (2g^4 C_F) B_4^0(1_d, 3_u, 4_{\bar{u}}, 2_{\bar{d}}), \quad B_4^u = B_2^u (2g^4 C_F) B_4^0(1_u, 3_d, 4_{\bar{d}}, 2_{\bar{u}}), \quad (3.66)$$

represent squared matrix elements involving only a single Born coupling. The term  $k_I$  partitions the full matrix-element correction, including interference, over both Born states,

$$k_I^{du} = \frac{B_4}{B_4^d + B_4^u} = 1 + \frac{B_4^{du}}{B_4^d + B_4^u}, \quad (3.67)$$

where  $B_4^{du}$  is the pure interference term in the squared matrix element appearing in the top line of fig. 6. This term is proportional to the mixed  $Z$ -quark couplings and to the four-quark antenna function dubbed  $\hat{B}_4^0$  of ref. [36].

For same-flavour  $Z \rightarrow q\bar{q}q\bar{q}$ , we use the identical-flavour four-parton matrix element in the definition of the interference factor,

$$k_I^{qq} = \frac{B_4^0(1_q, 3_q, 4_{\bar{q}}, 2_{\bar{q}}) + B_4^0(3_q, 1_q, 2_{\bar{q}}, 4_{\bar{q}}) - \frac{2}{N_C} [C_4^0(1_q, 3_q, 4_{\bar{q}}, 2_{\bar{q}}) + C_4^0(2_{\bar{q}}, 4_{\bar{q}}, 3_q, 1_q)]}{B_4^0(1_q, 3_q, 4_{\bar{q}}, 2_{\bar{q}}) + B_4^0(3_q, 1_q, 2_{\bar{q}}, 4_{\bar{q}})}, \quad (3.68)$$

where  $C_4^0$  is the same-flavour four-quark interference function given in ref. [36]. (For a strict leading-colour treatment one could leave out the  $C_4^0$  terms, resulting in  $k_I^{qq} = 1$ , but in the context of reducing matching uncertainties as much as possible we may as well include them here.) Following the notation of ref. [36], the arguments in  $B_4^0$  make the singularity explicit as  $3_q||4_{\bar{q}}$  in the first term and  $1_q||2_{\bar{q}}$  in the second.

Additionally, for each Born flavour channel, the matched NLO 3-jet rate must incorporate the  $k_I$  correction factor as well, inclusive over all flavours. Thus, we apply a different  $V_3^O$  depending on the generated Born flavour channel. That flavour-dependent  $V_{3q}^O$  is given by:

$$V_{3q}^O = 2\text{Re}[M_{3q}^1 M_{3q}^{0*}] + \int_{\hat{t}_3 > t_4} d\Phi_4 \left[ \mathbf{B}_2^q (2g^4 C_F) N_C A_4^0 + \mathbf{B}_4^{q(\text{id.})} + \sum_{q' \neq q}^{n_f} k_I^{qq'} \mathbf{B}_4^q \right] \delta^{(5)}(\Phi_3 - \hat{\Phi}_3(\Phi_4)). \quad (3.69)$$

We follow up with three additional comments on this procedure.

1. We note that, since all the terms in the denominator of  $k_I^{qq'}$  are positive definite, there is no risk of accidental cancellations causing vanishing denominators here, and since the numerator is also positive definite, the factor  $k_I$  is strictly positive and bounded.
2. In the following we focus on the  $N_F$  piece of  $V_{3q}^O$  only. Both the identical-flavour  $1/N_C$  correction in eq. (3.68) as well as the mixed-coupling interference term in eq. (3.67) yield finite contributions to  $V_{3q}^O$ . This is because the 3-parton configuration is resolved by construction, and both contributions yield finite results. This can also be seen by inspecting the structure of virtual corrections, see appendix B, and realising that in the quark sector the singularity is solely proportional to  $N_F$ .
3. The definition of “unclusterable” Born partons is valid not only for quark flavours, but also for Born gluons. Thus, in a  $H \rightarrow gg$  Born-level event, no clusterings to states involving fewer than two gluons would be considered by the sector algorithm. Or, if one were to start from  $Z \rightarrow q\bar{q}g$  events for some reason, no clusterings to states involving fewer than one gluon and one quark-antiquark pair of the requisite flavour would be considered. This makes the (unmatched) shower off a given Born state *independent* of the existence of any other Born states, i.e., universal, which we

consider a desirable property.<sup>8</sup> The matching then accounts for interferences between them, up to the matched order.

### 3.2.2 Sector resolution for $g \rightarrow q\bar{q}$ splittings

As was shown in the first sector-shower study [28], it is necessary to pick a slightly modified form of the sector resolution variable for  $g \rightarrow q\bar{q}$  splittings. The reason is that, while sector antenna functions for gluon emissions are symmetrised so that they contain also the collinear terms of the neighbouring antenna (and hence the full, symmetric  $p_{gg}(x)$ ), the equivalent for a  $gg \rightarrow \bar{q}qg$  antenna would have to include the collinear terms from a neighbouring  $qg$  gluon-emission antenna. Instead, the choice made in sector-shower implementations so far has therefore been to keep only the genuine  $g \rightarrow q\bar{q}$  gluon-splitting terms in the gluon-splitting antennae. But one must then modify the sector boundaries so that the neighbouring  $qg$  sector covers the entire  $qg$ -collinear region.

This is achieved by defining the sector resolution variable as follows [28, 31]:

$$Q_{\text{res}}^2 = \begin{cases} \frac{s_{ij}s_{jk}}{s_{IK}} = t_{[j]/ik}, & \text{if } j \text{ is a gluon} \\ s_{ij}\sqrt{\frac{s_{jk}}{s_{IK}}}, & \text{if } i, j \text{ is a same-flavour } q\bar{q} \text{ pair} \end{cases}, \quad (3.70)$$

where  $s_{ij} \equiv 2p_i \cdot p_j$ .

### 3.2.3 Sector subtraction for $g \rightarrow q\bar{q}$

In this section we present the matching formula in the sector subtraction construction following the same steps as in sec. 3.1. In the  $N_F$  channel we have the following

$$I_{3 \leftarrow 4}^{A, N_F} = \mathbb{B}_3 \frac{g^2 N_F}{A_3^0(\hat{1}_q, \hat{3}_g, \hat{2}_{\bar{q}})} \int_{\hat{t}_3 > t_{4A}} d\Phi_{+1}^A \Theta(Q_{\text{res}, B}^2 - Q_{\text{res}, A}^2) B_4^0. \quad (3.71)$$

In the case of quarks, as explained above, the sector resolution variable  $Q_{\text{res}}^2$  is different than that of gluon emissions. Nevertheless, at the 4-quark level, the *sector constraint*  $\Theta(Q_{\text{res}, B}^2 - Q_{\text{res}, A}^2)$  is identical to the gluon emission case  $\Theta(t_{4B} > t_{4A})$  because we consider only massless quarks. Therefore we use the same notation  $t_{4A/B}$ .

In order to construct a proper counter-term, we just need to realise that in the iterated (ordered)  $2 \mapsto 3$  limit, we have a  $q\bar{q} \rightarrow q\bar{q}g$  splitting followed by a  $g \rightarrow q'\bar{q}'$  splitting. Therefore, a proper counter-term must recover the full splitting function  $p_{qg}$ , i.e.

$$p_{qg}(z, \epsilon) = \frac{z^2 + (1-z)^2 - \epsilon}{(1-\epsilon)}. \quad (3.72)$$

---

<sup>8</sup>In the context of matching across different Born states, it can also be instructive to consider matching across  $H \rightarrow b\bar{b}, c\bar{c}$ , and in principle also  $s\bar{s}$  and lighter-quark Born states since, unlike the  $Z$  case, these have greatly different Born-level couplings. One would like a procedure that remains well-behaved and stable also for such cases, with matching factors mostly of order unity. (In the case of Higgs decays,  $H \rightarrow gg$  Born states would of course also need to be included for a complete matching, and contributions from hadronic  $H \rightarrow VV^*$  channels could be relevant too. Here, we restrict our attention to decays involving only  $q\bar{q}H$  couplings.)

We note that  $p_{qg}$  contains *twice* the pole structure found in the real-virtual term. Similarly to the case of gluon emission, we restrict the subtraction term to the singular region  $y_{13} < 1/2$ , which is sufficient to isolate the correct pole structure. We construct the following counter-term, which encodes the full  $p_{qg}(z, \epsilon)$  splitting function,<sup>9</sup>

$$E_3^{s0}(1_q, 3_{q'}, 4_{\bar{q}'}) = \frac{1}{s_{134}} \left( \frac{y_{13}^2 + y_{14}^2 - \epsilon}{(1 - \epsilon)y_{34}} + y_{13} + y_{14} \right). \quad (3.73)$$

We can now write down the equivalent of eq. (3.55), *viz.*

$$\begin{aligned} I_{3 \leftarrow 4}^{A, N_F} &= \mathbf{B}_3 \left( \frac{\alpha_s N_F}{2\pi} \right) \left( \frac{\hat{y}_{qg}^{-\epsilon}}{2} \left( -\frac{1}{3\epsilon} - \frac{13}{12} + \frac{\ln 2}{3} \right) - \mathcal{F}^{N_F}(\hat{y}_{g\bar{q}}) \right) \\ &+ \mathbf{B}_3 \left( \frac{\alpha_s N_F}{2\pi} \right) \left( w_{\text{RS}}^{A, N_F}(\hat{y}_{qg}, \hat{y}_{g\bar{q}}) + \mathcal{I}^{A, N_F}(\hat{y}_{qg}, \hat{y}_{g\bar{q}}) \right), \end{aligned} \quad (3.74)$$

where we defined:

$$w_{\text{RS}}^{A, N_F} = \frac{8\pi^2}{A_3^0(\hat{1}_q, \hat{3}_g, \hat{2}_{\bar{q}})} \int_{\hat{t}_3 > t_{4A}} d\Phi_{+1}^A \Theta(t_{4B} - t_{4A}) \left[ B_4^0 - A_3^0(\hat{1}_q, \hat{3}_g, \hat{2}_{\bar{q}}) E_3^{s0} \Theta\left(y_{13} < \frac{1}{2}\right) \right], \quad (3.75)$$

and

$$\mathcal{I}^{A, N_F} = 8\pi^2 \int_{\hat{t}_3 > t_{4A}} d\Phi_{+1}^A E_3^{s0} \Theta\left(y_{13} < \frac{1}{2}\right) \left[ \Theta(t_{4B} - t_{4A}) - 1 \right]. \quad (3.76)$$

Therefore, in complete analogy to eq. (3.61), we write

$$v_{N_F}^{\text{NLO}} = \left( \frac{\alpha_s N_F}{2\pi} \right) \left( w_{\text{RS}}^{A, N_F} + \mathcal{I}^{A, N_F} + w_{\text{RS}}^{A, N_F} + \mathcal{I}^{A, N_F} + w_{\mathcal{V}}^{N_F} \right), \quad (3.77)$$

with the results plotted in fig. 7. The logarithmic structure of  $w_{\mathcal{V}}^{N_F}$  has the following form

$$\lim_{\tau_3 \rightarrow 0} w_{\mathcal{V}}^{N_F} \rightarrow \frac{1}{3} \ln \tau_3 + \frac{\ln 2}{3} - \frac{11}{72}. \quad (3.78)$$

### 3.3 The renormalisation terms

We are now ready to present the final NLO coefficient  $A_{2 \rightarrow 3}^{\text{NLO}}$ , which enters our matching formula. Substituting eqs. (2.13) and (3.60) in eq. (3.22), we have

$$A_{2 \rightarrow 3}^{\text{NLO}} = A_{2 \rightarrow 3}^{\text{LO}} K^{\text{NLO}}, \quad (3.79)$$

$$K^{\text{NLO}} = \frac{1 - \Delta_2^1(m_Z^2, \hat{t}_3) + v_{N_C}^{\text{NLO}} + v_{N_F}^{\text{NLO}}}{1 + \frac{\alpha_s(m_Z)}{\pi}}, \quad (3.80)$$

where the denominator comes from our choice<sup>10</sup> to exactly reproduce the  $\mathbf{B}_2 + \mathbf{V}_2$  denominator in eq. (3.22), and we emphasise that  $\Delta_2^1$  in the numerator should be expanded to leading colour since  $v_{N_C}^{\text{NLO}}$  likewise does not include  $1/N_C^2$  corrections.

<sup>9</sup>Our counter-term differs from the 3-parton tree-level antenna  $E_3^0$  of refs. [36, 47] only by finite terms.

<sup>10</sup>This choice differs from that of ref. [32] at order  $\mathcal{O}(\alpha_s^2)$  in  $K^{\text{NLO}}$ , i.e. beyond the matched accuracy.

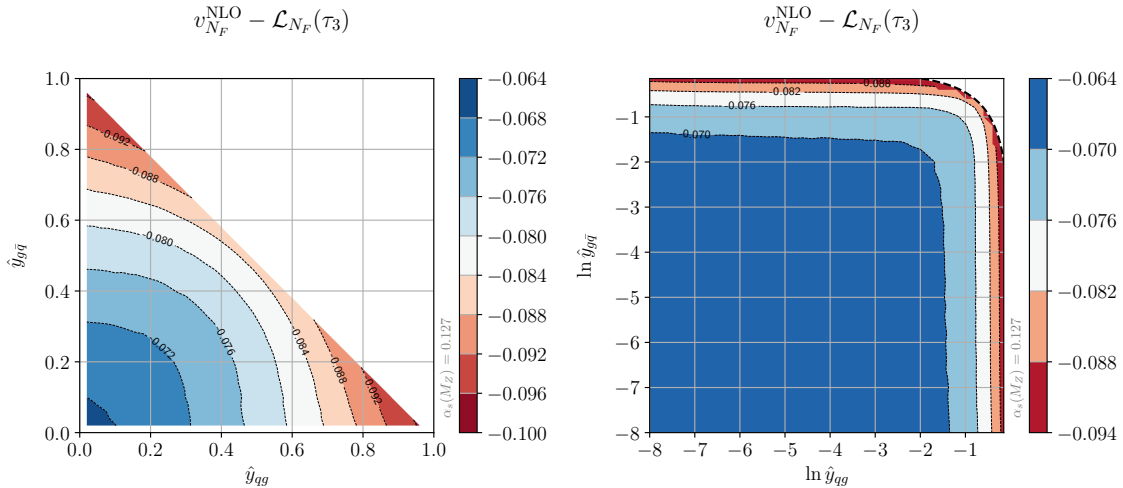


**Figure 7.** The result of the  $v_{N_F}^{\text{NLO}}$  factor as defined in eq. (3.77), where we subtract the log-enhanced terms of eq. (3.78),  $\mathcal{L}_{N_F}(\tau_3) = \frac{1}{3} \ln \tau_3$ .

In addition to the above, we need to account for the scale and scheme choices used for the strong coupling on the shower side. The iterated  $2 \mapsto 3$  shower evaluates the coupling at the scale proportional to the transverse momentum of the emission,  $\hat{t}_3 = \hat{y}_{gg}\hat{y}_{gq}m_Z^2 = \tau_3 m_Z^2$ , and additionally typically uses the CMW scheme [37]:

$$\alpha_s \rightarrow \alpha_s(\hat{t}_3) \left( 1 + \frac{\alpha_s(\hat{t}_3)}{2\pi} K_{\text{CMW}} \right). \quad (3.81)$$

On the fixed-order side, it is customary to set the renormalisation scale  $\mu_M = m_Z$ . We therefore need to subtract these two contributions in the NLO matching coefficient,

$$K_{\text{full}}^{\text{NLO}} = \frac{1 - \Delta_2^1(m_Z^2, \hat{t}_3) + v_{N_C}^{\text{NLO}} + v_{N_F}^{\text{NLO}} - \frac{\alpha_s}{2\pi} K_{\text{CMW}} + \frac{\alpha_s}{2\pi} b_0 \ln \tau_3}{1 + \frac{\alpha_s(m_Z)}{\pi}}, \quad (3.82)$$

with the two-loop cusp anomalous dimension and the one-loop coefficient of the  $\beta$ -function,

$$K_{\text{CMW}} = N_C \left( \frac{67}{18} - \frac{\pi^2}{6} \right) - \frac{5}{9} N_F, \quad b_0 = \frac{11N_C}{6} - \frac{N_F}{3}. \quad (3.83)$$

Inspection of eqs. (3.25), (3.62) and (3.78) reveals that in the limit  $\tau_3 \rightarrow 0$  all  $\ln \tau_3$  enhanced contributions cancel out in the result for  $K_{\text{full}}^{\text{NLO}}$ .

We note that the scale and scheme choice used for  $\alpha_s$  in the numerator of  $K_{\text{full}}^{\text{NLO}}$  is an  $\mathcal{O}(\alpha_s^3)$  ambiguity and is hence not fixed by the NNLO matching conditions. Either of the choices  $\mu^2 = \mu_M^2 = m_Z^2$  or  $\mu^2 = \hat{t}_3$  could be justified. As a pragmatic solution, pending further investigations, we advocate using the geometric mean,  $\mu^2 = \sqrt{\hat{t}_3} m_Z$ , with the two limiting values used for uncertainty estimates.

A further subtlety, which was also touched on in ref. [38], is what happens as the perturbative evolution in the shower crosses flavour thresholds, i.e., for  $\hat{t}_3 < m_b^2$  and for  $\hat{t}_3 < m_c^2$ . In the VINCIA shower, at each flavour threshold,

1. The phase space for gluon splittings,  $g \rightarrow Q\bar{Q}$ , closes. Hence the value of  $N_F$  for real splittings decreases by one.
2. The value of  $N_F$  used in the running of  $\alpha_s$  (including in the evaluation of the CMW factor) decreases by one. The running is matched across flavour thresholds so that it is continuous. Thus,  $\alpha_s^{N_F=5}(m_b^2) = \alpha_s^{N_F=4}(m_b^2)$  and  $\alpha_s^{N_F=4}(m_c^2) = \alpha_s^{N_F=3}(m_c^2)$ .

Consider the  $N_F$ -dependent term in the combination of the one-loop and real matrix elements in  $V_3^O$ ,

$$\frac{\alpha_s(m_Z^2)}{2\pi} \frac{N_F}{3} \ln \left[ \frac{\hat{t}_3}{m_Z^2} \right] \mathbf{B}_3, \quad (3.84)$$

with  $N_F = 5$  for a renormalisation scale  $\mu_M = m_Z$ . For values of the transverse momentum  $\sqrt{\hat{t}_3}$  below the  $b$ -quark mass, we “freeze” the contribution from the  $b$  quark,

$$\hat{t}_3 < m_b^2 : \quad \frac{\alpha_s(m_Z^2)}{2\pi} \left( \frac{4}{3} \ln \left[ \frac{\hat{t}_3}{m_Z^2} \right] + \frac{1}{3} \ln \left[ \frac{m_b^2}{m_Z^2} \right] \right) \mathbf{B}_3, \quad (3.85)$$

and similarly, below the  $c$ -quark threshold,

$$\hat{t}_3 < m_c^2 : \quad \frac{\alpha_s(m_Z^2)}{2\pi} \left( \frac{3}{3} \ln \left[ \frac{\hat{t}_3}{m_Z^2} \right] + \frac{1}{3} \ln \left[ \frac{m_b^2}{m_Z^2} \right] + \frac{1}{3} \ln \left[ \frac{m_c^2}{m_Z^2} \right] \right) \mathbf{B}_3. \quad (3.86)$$

This is equivalent to the structure that results from changing the running of the coupling across flavour thresholds, as is done by default in VINCIA. There is therefore no remainder from this modification.

## 4 Uncertainties

Any calculation is only as good as its uncertainty estimates. In the matching between NNLO perturbation theory and the sector shower, there are several sources of ambiguities which generate uncertainties starting from  $\mathcal{O}(\alpha_s^3)$  and  $\mathcal{O}(\alpha_s^2/N_C^2)$ . (The latter is due to the fact that we did not here include the virtual corrections at full colour.)

We note that leading QED/EW bremsstrahlung corrections can in principle be easily incorporated by enabling VINCIA’s multipole QED shower [48] or EW shower [49] modules, either of which can be interleaved with the NNLO-matched QCD shower. We do not believe achieving simultaneous NNLO QCD and NLO QED accuracy should present any conceptual difficulties but defer a detailed discussion of QED/EW matching in this framework to future work. Here, we focus on QCD uncertainties that are specifically due to the matching, on the interface between the fixed-order and shower calculations.

Starting with NLO matching, there are the well-known ambiguities between MC@NLO-type [12] and POWHEG-type [14] matching schemes. In our notation, an analogous difference can be induced by introducing a parameter  $\rho \in [-1, 2]$  in the definition of the tree-level matched antenna function,

$$A_{2 \rightarrow 3}^{\text{LO}} \rightarrow A_{2 \rightarrow 3}^{\text{LO}}(\rho) = A_{2 \rightarrow 3}^{\text{LO}} \frac{\mathbf{B}_2}{\mathbf{B}_2 + \rho \mathbf{V}_2}, \quad (4.1)$$



where  $\rho = 0$  yields the functional form of the matching from ref. [32]. Generalising this to NNLO matching the ambiguity moves one order higher,

$$A_{2\rightarrow 3}^{\text{NLO}} \rightarrow A_{2\rightarrow 3}^{\text{NLO}}(\rho) = A_{2\rightarrow 3}^{\text{NLO}} \frac{B_2 + V_2}{B_2 + V_2 + \rho_W W_2}. \quad (4.2)$$

We also introduce explicit  $\mathcal{O}(\alpha_s^3)$  ambiguities in the definitions of  $V_3$  and the tree-level four-parton antenna functions, via substitutions

$$V_3 \rightarrow V_3 \pm \left(\frac{\alpha_s}{2\pi}\right)^3 \rho_V, \quad (4.3)$$

$$B_4 \rightarrow B_4 \pm \left(\frac{\alpha_s}{2\pi}\right)^3 \rho_T, \quad (4.4)$$

with  $\rho_{V,T} = \mathcal{O}(1)$ .

For the scale definitions in the  $\alpha_s$  evaluations here, we again recommend taking the geometric mean of the pre- and post-branching scales as the central value, i.e.,  $\mu^2 = \sqrt{t_3} m_Z$  for  $V_3$  and  $\mu^2 = \sqrt{t_3 t_4}$  for  $B_4$  (and  $\mu^2 = t_4$  for direct  $2 \mapsto 4$  phase-space points). In addition to this, the renormalisation scale used for the explicit  $\alpha_s$  factors in  $K^{\text{NLO}}$  can be varied between  $t_3$  and  $m_Z$ , as was discussed above.

Finally, we propose to match on to conventional renormalisation-scale variations in the pure shower description by varying the renormalisation scale used to evaluate  $\alpha_s$  in  $A_{3\rightarrow 4}$  and  $A_{2\rightarrow 4}$  by a factor  $\propto 2$  around  $t_4$ .

## 5 Summary & Outlook

In this paper we derived the necessary matching conditions to achieve NNLO accuracy within the VINCIA sector shower algorithm, with the NLO 3-jet correction expanded to leading colour. We have built on the consistent inclusion of direct  $2 \mapsto 4$  branchings in the unordered phase space of the sector shower, following ref. [39]. In particular, we utilised the sector resolution variable to cleanly separate out the ordered phase space (populated by iterated  $2 \mapsto 3$  branchings) from the unordered one (produced by direct  $2 \mapsto 4$  branchings). The fixed-order jet rates used in the matching conditions were defined according to the ARCLUS  $3 \mapsto 2$  clustering algorithm [33]. This is especially convenient because VINCIA's sector resolution criterion aligns with the ARCLUS jet resolution.

The main result of this paper is the derivation and computation of the  $K_{\text{NLO}}$  3-jet matching coefficient given in eq. (3.82). The major difficulty in the evaluation of this factor consists in the presence of the sector constraint in the 4-parton phase space. We devised a subtraction procedure optimised to achieve high accuracy on the numerical component of  $K_{\text{NLO}}$ . This enables the matching coefficient to be efficiently included in VINCIA, thereby delivering the last missing ingredient for NNLO matching in our shower.

In a follow-up paper, we plan to present phenomenological results for hadronic  $Z$  decays, in combination with a public release of the VINCIA code implementing our method. We believe that our procedure can be generalised to more elaborate processes with minimal effort. We leave to future work the formulation of subleading-colour effects, initial-state radiation, and NNLO matching to final states with more than two hard legs.

## Acknowledgements

We thank J. Altmann for comments on the manuscript. BKE and PS are supported by the Australian Research Council under grant DP220103512. LS is supported by the Australian Research Council under grant DE230100867. We are grateful to the Rudolf Peierls Centre for Theoretical Physics, University of Oxford, and to the Aspen Center for Physics, Colorado, for hospitality and stimulating working environments during discussions of this work. In Oxford, PS was supported by a Royal Society Wolfson Visiting Fellowship RSWVF\R1\231006. The Aspen Center for Physics is supported by National Science Foundation grant PHY-2210452.

## A The function $\mathcal{F}(x)$

Here we list the finite function that appears in eq. (3.53), which results from the ordering restriction  $t_{4A} < \hat{t}_3$ . We first define an auxiliary function

$$\begin{aligned} \mathcal{G}^{N_C}(y) = & \frac{31y}{6} + \frac{3y^2}{4} - \frac{y^3}{9} + \frac{y^4}{16} + \frac{\pi^2}{3} - \frac{11 \tanh^{-1}(y)}{3} - 2 \ln^2 2 + \frac{3}{2} \ln(1-y) \\ & + \ln^2(1-y) - 2 \ln(1-y) \ln(1+y) + \ln\left(\frac{16}{1+y}\right) \ln(1+y) - 4 \text{Li}_2\left(\frac{1+y}{2}\right), \end{aligned} \quad (\text{A.1})$$

and thus

$$\mathcal{F}^{N_C}(x) = \frac{1}{2} \Theta\left(x \leq \frac{1}{4}\right) \mathcal{G}^{N_C}(\sqrt{1-4x}). \quad (\text{A.2})$$

Similarly for the  $N_F$  contribution we obtain

$$\mathcal{G}^{N_F}(y) = \frac{1}{72} \left( y(-66 - 9y + 8y^2) + 6(3y^2 - 7) \ln(1-y) + 24 \ln(1+y) \right).$$

## B Virtual corrections

Using the notation of ref. [36], virtual corrections can easily be obtained from the 1-loop  $q\bar{q}$  antenna function,  $A_3^1$ , and the integrated one-loop  $q\bar{q}$  antenna function,  $\mathcal{A}_2^1$ . We can express the real-virtual contribution as follows:

$$\begin{aligned} 2\text{Re}[M_3^1 M_3^{0*}] = & \mathbb{B}_3 \left( \frac{\mu_R^2}{m_Z^2} \right)^\epsilon m_Z^{2\epsilon} \left[ \left( \frac{\alpha_s N_C}{2\pi} \right) \left( \frac{A_3^1(\hat{1}_q, \hat{3}_g, \hat{2}_{\bar{q}})}{A_3^0(\hat{1}_q, \hat{3}_g, \hat{2}_{\bar{q}})} + \mathcal{A}_2^1(m_Z^2) \right) \right. \\ & \left. + \left( \frac{\alpha_s N_F}{2\pi} \right) \frac{\hat{A}_3^1(\hat{1}_q, \hat{3}_g, \hat{2}_{\bar{q}})}{A_3^0(\hat{1}_q, \hat{3}_g, \hat{2}_{\bar{q}})} \right], \end{aligned}$$

where  $A_3^1$  is the  $q\bar{q}g$  antenna function at one loop,  $\mathcal{A}_2^1$  is the integrated one-loop  $q\bar{q}$  antenna function and  $\hat{A}_3^1$  is the fermionic one-loop contribution. It is best to define the following

dimensionless functions,

$$\begin{aligned}
T_3^0(\hat{y}_{qg}, \hat{y}_{g\bar{q}}) &= \frac{2(1 - \hat{y}_{qg} - \hat{y}_{g\bar{q}})}{\hat{y}_{qg}\hat{y}_{g\bar{q}}} + \frac{\hat{y}_{qg}}{\hat{y}_{g\bar{q}}} + \frac{\hat{y}_{g\bar{q}}}{\hat{y}_{qg}}, \\
T_3^1(\hat{y}_{qg}, \hat{y}_{g\bar{q}}) &= \frac{1}{2\hat{y}_{qg}} - \frac{\hat{y}_{qg}}{2(1 - \hat{y}_{g\bar{q}})} + \ln(\hat{y}_{qg}) \left( 2 - \frac{\hat{y}_{qg}\hat{y}_{g\bar{q}}}{2(1 - \hat{y}_{qg})^2} + 2\frac{\hat{y}_{qg} - \hat{y}_{g\bar{q}}}{1 - \hat{y}_{qg}} \right) + \hat{y}_{qg} \leftrightarrow \hat{y}_{g\bar{q}}.
\end{aligned} \tag{B.1}$$

Using the relevant expressions from [36] we obtain

$$\begin{aligned}
2\text{Re}[M_3^1 M_3^{0*}] &= \\
\mathbf{B}_3 \left( \frac{\alpha_s N_C}{2\pi} \right) \left( \frac{\mu_R^2}{m_Z^2} \right)^\epsilon &\left[ -\frac{2}{\epsilon^2} - \frac{10}{3\epsilon} + \frac{\ln \hat{y}_{qg} + \ln \hat{y}_{g\bar{q}}}{\epsilon} - 4 + \frac{7\pi^2}{6} - \frac{1}{2} \ln^2 \hat{y}_{qg} - \frac{1}{2} \ln^2 \hat{y}_{g\bar{q}} \right. \\
&\left. - R(\hat{y}_{qg}, \hat{y}_{g\bar{q}}) + \frac{T_3^1(\hat{y}_{qg}, \hat{y}_{g\bar{q}})}{T_3^0(\hat{y}_{qg}, \hat{y}_{g\bar{q}})} \right] + \mathbf{B}_3 \left( \frac{\alpha_s N_F}{2\pi} \right) \left( \frac{\mu_R^2}{m_Z^2} \right)^\epsilon \frac{1}{3\epsilon}, \tag{B.2}
\end{aligned}$$

where  $R(\hat{y}_{qg}, \hat{y}_{g\bar{q}})$  is given in ref. [36]:

$$R(x, y) = \ln x \ln y - \ln x \ln(1 - x) - \ln y \ln(1 - y) + \frac{\pi^2}{6} - \text{Li}_2(x) - \text{Li}_2(y). \tag{B.3}$$

### C NLO 3-jet matching with global subtraction

As an alternative to the directly constructed sector subtraction presented in the main body of the paper, we also investigated a variant based on global antenna subtraction. In our studies, this turned out to be less numerically efficient, but we present it here for future reference.

Using that the pole structure of  $2\text{Re}[M_3^1 M_3^{0*}]$  should be reproduced by integrals over global quark-gluon antenna-subtraction terms, we first rewrite

$$\int_{\hat{t}_3 > t_{4A}} d\Phi_{+1}^A \left( \Theta(t_{4B} - t_{4A}) \mathbf{B}_4 - \mathbf{B}_3 g^2 N_C d_3^A \right) + \mathbf{B}_3 g^2 N_C \overbrace{\int_{\hat{t}_3 > t_{4A}} d\Phi_{+1}^A d_3^A}^{I_{3A}^{\text{gO}}} + A \leftrightarrow B, \tag{C.1}$$

where  $d_3^A$  can be chosen, e.g., to be the GGG sub-antenna function for gluon emission off a quark-gluon antenna [36] (modulo colour and coupling factors), *viz.*

$$d_3^A(1_q, 3_g, 4_g) = \frac{1}{s_{134}} \left( \frac{2y_{14}}{y_{13}y_{34}} + \frac{y_{34}}{y_{13}} - y_{34} + \frac{y_{14}y_{13}}{y_{34}} + \frac{5}{2} + \frac{y_{34}}{2} - \epsilon \frac{y_{34}}{y_{13}} \right). \tag{C.2}$$

The subtraction term, i.e.  $I_{3A}^{\text{gO}}$ , then only differs from the standard global NLO antenna-

subtraction integrals by the restriction to  $\hat{t}_3 > t_{4A}$ . It is given by:

$$I_{3A}^{\text{gO}} = g^2 N_C \int_{\hat{t}_3 > t_4} d\Phi_{+1}^A d_3^A \quad (\text{C.3})$$

$$= g^2 N_C \left[ \frac{\mathcal{D}_3^0(\epsilon, \hat{s}_{q\bar{q}})}{2} - \int_{t_4 > \hat{t}_3} d\Phi_{+1}^A d_3^A \right] \quad (\text{C.4})$$

$$\begin{aligned} &= \frac{\alpha_s N_C}{2\pi} \left( -2\mathbf{I}_{q\bar{q}}(\epsilon, \hat{s}_{q\bar{q}}) + \frac{17}{3} \right) \\ &+ \frac{\alpha_s N_C}{2\pi} \Theta \left( \hat{y}_{q\bar{q}} < \frac{1}{4} \right) \left[ \frac{7x^3}{72} - \frac{285x}{72} + \left( \frac{285}{72} - \frac{45}{72}x^2 \right) \tanh^{-1}(x) \right. \\ &\quad \left. + \frac{1}{2} \ln(1-x) \ln \frac{4}{1-x} + \frac{1}{2} \ln \frac{1+x}{4} \ln(1+x) \right. \\ &\quad \left. - \text{Li}_2 \left( \frac{1-x}{2} \right) + \text{Li}_2 \left( \frac{1+x}{2} \right) \right], \quad (\text{C.5}) \end{aligned}$$

with  $x = \sqrt{1 - 4\hat{y}_{q\bar{q}}}$ . The integrated tree-level antenna function,  $\mathcal{D}_3^0$ , and its decomposition into pole ( $\mathbf{I}_{q\bar{q}}$ ) and finite terms is given in [36]. The finite terms of eq. (C.5) that arise from the restriction  $t_4 > \hat{t}_3$  would be absent in a standard fixed-order context. The expression for the matching coefficient  $\mathbf{V}_3^{\text{O}}$  is then

$$\begin{aligned} \mathbf{V}_3^{\text{O}} &= \overbrace{2\text{Re}[M_3^1 M_3^{0*}]}^{\text{finite}} + \left( I_{3A}^{\text{gO}} + I_{3B}^{\text{gO}} \right) \mathbf{B}_3 \quad (\text{C.6}) \\ &+ \int_{\hat{t}_3 > t_{4A}} d\Phi_{+1}^A \left( \Theta(t_{4B} - t_{4A}) \mathbf{B}_4 - \mathbf{B}_3 g^2 N_C d_3^A \right) + A \leftrightarrow B. \end{aligned}$$

However, the terms on the second line in eq. (C.6) cannot yet be integrated numerically. This is because the term featuring the global antenna function does not provide a *local* subtraction (point-by-point) in phase space. This is the main difference between this approach and that based on sector subtraction presented in the body of the paper. We can still leverage the insights from sec. 3.1 to rearrange the computation and make it amenable to numerical integration. The analysis of the sector constraint in sec. 3.1 proved that the gluon-gluon collinear singularity is contained in the region  $y_{13} < 1/2$  as depicted in fig. 1.

Given that the sub-antenna function  $d_3^A$  represents a smooth partial-fractioning of  $p_{g\bar{g}}$ ,  $d_3^A$  does not contain the full singular behaviour of  $A_4^0$ . Therefore, we can remove the gluon-gluon collinear limit of  $d_3^A$  and replace it instead with the full splitting function  $p_{g\bar{g}}$  in the

region  $y_{13} < 1/2$ . Therefore, we obtain:

$$\begin{aligned}
V_3^{\text{O}} &= \overbrace{2\text{Re}[M_3^1 M_3^{0*}] + \left(I_{3A}^{\text{gO}} + I_{3B}^{\text{gO}}\right) \mathbf{B}_3}^{\text{finite}} \\
&+ \mathbf{B}_3 g^2 N_C \int_{\hat{t}_3 > t_{4A}} d\Phi_{+1}^A \left[ \frac{1}{s_{34}} p_{gg}(y_{13}) \Theta\left(y_{13} < \frac{1}{2}\right) - \tilde{d}_3^A \right] \\
&+ \int_{\hat{t}_3 > t_{4A}} d\Phi_{+1}^A \left( \Theta(t_{4B} - t_{4A}) \mathbf{B}_4 - \mathbf{B}_3 g^2 N_C \left[ \frac{1}{s_{34}} p_{gg}(y_{13}) \Theta\left(y_{13} < \frac{1}{2}\right) + (d_3^A - \tilde{d}_3^A) \right] \right) \\
&+ A \leftrightarrow B,
\end{aligned} \tag{C.7}$$

where

$$p_{gg}(y_{13}) = \frac{2y_{13}}{(1-y_{13})} + \frac{2(1-y_{13})}{y_{13}} + 2y_{13}(1-y_{13}), \tag{C.8}$$

$$\tilde{d}_3^A = \frac{1}{s_{34}} \left( \frac{(1-y_{13})}{y_{13}} + y_{13}(1-y_{13}) \right). \tag{C.9}$$

The last line in eq. (C.10) is now amenable to numerical integration. The second line in eq. (C.10) is finite, albeit it needs to be evaluated in  $D = 4 - 2\epsilon$  to cancel the potential  $y_{34} \rightarrow 0$  singularity before taking the limit  $\epsilon = 0$ . Using the phase space given in eq. (3.31), we obtain:

$$\begin{aligned}
V_3^{\text{O}} &= \overbrace{2\text{Re}[M_3^1 M_3^{0*}] + \left(I_{3A}^{\text{gO}} + I_{3B}^{\text{gO}}\right) \mathbf{B}_3}^{\text{finite}} \\
&+ \mathbf{B}_3 \frac{\alpha_s N_C}{2\pi} \frac{1}{2} \left( \frac{\pi^2}{6} - \frac{1}{24} - \frac{11 \ln 2}{6} \right) \\
&+ \int_{\hat{t}_3 > t_{4A}} d\Phi_{+1}^A \left( \Theta(t_{4B} - t_{4A}) \mathbf{B}_4 - \mathbf{B}_3 g^2 N_C \left[ \frac{1}{s_{34}} p_{gg}(y_{13}) \Theta\left(y_{13} < \frac{1}{2}\right) + (d_3^A - \tilde{d}_3^A) \right] \right) \\
&+ A \leftrightarrow B.
\end{aligned} \tag{C.10}$$

Finally, we have checked explicitly that the above approach yields identical results to the sector subtraction approach presented in the body of the article.

## References

- [1] M. Dasgupta, F.A. Dreyer, K. Hamilton, P.F. Monni, G.P. Salam and G. Soyez, *Parton showers beyond leading logarithmic accuracy*, *Phys. Rev. Lett.* **125** (2020) 052002 [[2002.11114](#)].
- [2] M. van Beekveld, S. Ferrario Ravasio, K. Hamilton, G.P. Salam, A. Soto-Ontoso, G. Soyez et al., *PanScales showers for hadron collisions: all-order validation*, *JHEP* **11** (2022) 020 [[2207.09467](#)].

- [3] M. van Beekveld and S. Ferrario Ravasio, *Next-to-leading-logarithmic PanScales showers for Deep Inelastic Scattering and Vector Boson Fusion*, *JHEP* **02** (2024) 001 [2305.08645].
- [4] J.R. Forshaw, J. Holguin and S. Plätzer, *Building a consistent parton shower*, *JHEP* **09** (2020) 014 [2003.06400].
- [5] Z. Nagy and D.E. Soper, *Summations by parton showers of large logarithms in electron-positron annihilation*, **2011.04777**.
- [6] Z. Nagy and D.E. Soper, *Summations of large logarithms by parton showers*, *Phys. Rev. D* **104** (2021) 054049 [2011.04773].
- [7] F. Herren, S. Höche, F. Krauss, D. Reichelt and M. Schoenherr, *A new approach to color-coherent parton evolution*, *JHEP* **10** (2023) 091 [2208.06057].
- [8] B. Assi and S. Höche, *New approach to QCD final-state evolution in processes with massive partons*, *Phys. Rev. D* **109** (2024) 114008 [2307.00728].
- [9] C.T. Preuss, *A partitioned dipole-antenna shower with improved transverse recoil*, *JHEP* **07** (2024) 161 [2403.19452].
- [10] S. Ferrario Ravasio, K. Hamilton, A. Karlberg, G.P. Salam, L. Scyboz and G. Soyez, *Parton Showering with Higher Logarithmic Accuracy for Soft Emissions*, *Phys. Rev. Lett.* **131** (2023) 161906 [2307.11142].
- [11] M. van Beekveld et al., *A new standard for the logarithmic accuracy of parton showers*, **2406.02661**.
- [12] S. Frixione and B.R. Webber, *Matching NLO QCD computations and parton shower simulations*, *JHEP* **06** (2002) 029 [hep-ph/0204244].
- [13] P. Nason, *A New method for combining NLO QCD with shower Monte Carlo algorithms*, *JHEP* **11** (2004) 040 [hep-ph/0409146].
- [14] S. Frixione, P. Nason and C. Oleari, *Matching NLO QCD computations with Parton Shower simulations: the POWHEG method*, *JHEP* **11** (2007) 070 [0709.2092].
- [15] S. Jadach, W. Płaczek, S. Sapeta, A. Siódmok and M. Skrzypek, *Matching NLO QCD with parton shower in Monte Carlo scheme — the KrkNLO method*, *JHEP* **10** (2015) 052 [1503.06849].
- [16] P. Sarmah, A. Siódmok and J. Whitehead, *KrkNLO matching for colour-singlet processes*, **2409.16417**.
- [17] P. Nason and G.P. Salam, *Multiplicative-accumulative matching of NLO calculations with parton showers*, *JHEP* **01** (2022) 067 [2111.03553].
- [18] K. Hamilton, P. Nason, E. Re and G. Zanderighi, *NNLOPS simulation of Higgs boson production*, *JHEP* **10** (2013) 222 [1309.0017].
- [19] L. Lönnblad and S. Prestel, *Merging Multi-leg NLO Matrix Elements with Parton Showers*, *JHEP* **03** (2013) 166 [1211.7278].
- [20] S. Höche, Y. Li and S. Prestel, *Drell-Yan lepton pair production at NNLO QCD with parton showers*, *Phys. Rev. D* **91** (2015) 074015 [1405.3607].
- [21] P.F. Monni, P. Nason, E. Re, M. Wiesemann and G. Zanderighi, *MiNNLO<sub>PS</sub>: a new method to match NNLO QCD to parton showers*, *JHEP* **05** (2020) 143 [1908.06987].

- [22] S. Alioli, C.W. Bauer, C. Berggren, F.J. Tackmann, J.R. Walsh and S. Zuberi, *Matching Fully Differential NNLO Calculations and Parton Showers*, *JHEP* **06** (2014) 089 [[1311.0286](#)].
- [23] R. Corke and T. Sjostrand, *Improved Parton Showers at Large Transverse Momenta*, *Eur. Phys. J. C* **69** (2010) 1 [[1003.2384](#)].
- [24] K. Hamilton, A. Karlberg, G.P. Salam, L. Scyboz and R. Verheyen, *Soft spin correlations in final-state parton showers*, *JHEP* **03** (2022) 193 [[2111.01161](#)].
- [25] S. Catani, F. Krauss, R. Kuhn and B.R. Webber, *QCD matrix elements + parton showers*, *JHEP* **11** (2001) 063 [[hep-ph/0109231](#)].
- [26] S. Hoche, F. Krauss, M. Schonherr and F. Siegert, *Automating the POWHEG method in Sherpa*, *JHEP* **04** (2011) 024 [[1008.5399](#)].
- [27] S. Platzer and S. Gieseke, *Dipole Showers and Automated NLO Matching in Herwig++*, *Eur. Phys. J. C* **72** (2012) 2187 [[1109.6256](#)].
- [28] J.J. Lopez-Villarejo and P.Z. Skands, *Efficient Matrix-Element Matching with Sector Showers*, *JHEP* **11** (2011) 150 [[1109.3608](#)].
- [29] A.J. Larkoski, J.J. Lopez-Villarejo and P. Skands, *Helicity-Dependent Showers and Matching with VINCIA*, *Phys. Rev. D* **87** (2013) 054033 [[1301.0933](#)].
- [30] N. Fischer, S. Prestel, M. Ritzmann and P. Skands, *Vincia for Hadron Colliders*, *Eur. Phys. J. C* **76** (2016) 589 [[1605.06142](#)].
- [31] H. Brooks, C.T. Preuss and P. Skands, *Sector Showers for Hadron Collisions*, *JHEP* **07** (2020) 032 [[2003.00702](#)].
- [32] J.M. Campbell, S. Höche, H.T. Li, C.T. Preuss and P. Skands, *Towards NNLO+PS matching with sector showers*, *Phys. Lett. B* **836** (2023) 137614 [[2108.07133](#)].
- [33] L. Lönnblad, *ARCLUS: A New jet clustering algorithm inspired by the color dipole model*, *Z. Phys. C* **58** (1993) 471.
- [34] R.K. Ellis, D.A. Ross and A.E. Terrano, *The Perturbative Calculation of Jet Structure in  $e+e-$  Annihilation*, *Nucl. Phys. B* **178** (1981) 421.
- [35] E. Norrbin and T. Sjostrand, *QCD radiation off heavy particles*, *Nucl. Phys. B* **603** (2001) 297 [[hep-ph/0010012](#)].
- [36] A. Gehrmann-De Ridder, T. Gehrmann and E.W.N. Glover, *Antenna subtraction at NNLO*, *JHEP* **09** (2005) 056 [[hep-ph/0505111](#)].
- [37] S. Catani, B.R. Webber and G. Marchesini, *QCD coherent branching and semiinclusive processes at large  $x$* , *Nucl. Phys. B* **349** (1991) 635.
- [38] L. Hartgring, E. Laenen and P. Skands, *Antenna Showers with One-Loop Matrix Elements*, *JHEP* **10** (2013) 127 [[1303.4974](#)].
- [39] H.T. Li and P. Skands, *A framework for second-order parton showers*, *Phys. Lett. B* **771** (2017) 59 [[1611.00013](#)].
- [40] W.T. Giele, D.A. Kosower and P.Z. Skands, *Higher-Order Corrections to Timelike Jets*, *Phys. Rev. D* **84** (2011) 054003 [[1102.2126](#)].
- [41] L. Lönnblad, *ARIADNE version 4: A Program for simulation of QCD cascades implementing the color dipole model*, *Comput. Phys. Commun.* **71** (1992) 15.

- [42] D.A. Kosower, *Antenna factorization in strongly ordered limits*, *Phys. Rev. D* **71** (2005) 045016 [[hep-ph/0311272](#)].
- [43] S. Catani and M.H. Seymour, *The Dipole formalism for the calculation of QCD jet cross-sections at next-to-leading order*, *Phys. Lett. B* **378** (1996) 287 [[hep-ph/9602277](#)].
- [44] O. Braun-White, N. Glover and C.T. Preuss, *A general algorithm to build real-radiation antenna functions for higher-order calculations*, *JHEP* **06** (2023) 065 [[2302.12787](#)].
- [45] S. Weinzierl and D.A. Kosower, *QCD corrections to four jet production and three jet structure in  $e^+ e^-$  annihilation*, *Phys. Rev. D* **60** (1999) 054028 [[hep-ph/9901277](#)].
- [46] H. Brooks and C.T. Preuss, *Efficient multi-jet merging with the Vincia sector shower*, *Comput. Phys. Commun.* **264** (2021) 107985 [[2008.09468](#)].
- [47] A. Gehrmann-De Ridder, T. Gehrmann and E.W.N. Glover, *Quark-gluon antenna functions from neutralino decay*, *Phys. Lett. B* **612** (2005) 36 [[hep-ph/0501291](#)].
- [48] P. Skands and R. Verheyen, *Multipole photon radiation in the Vincia parton shower*, *Phys. Lett. B* **811** (2020) 135878 [[2002.04939](#)].
- [49] H. Brooks, P. Skands and R. Verheyen, *Interleaved resonance decays and electroweak radiation in the Vincia parton shower*, *SciPost Phys.* **12** (2022) 101 [[2108.10786](#)].